

Natural hydrogen seeps as analogues to inform monitoring of engineered geological hydrogen storage



Christopher J. McMahon^{1*}, Jennifer J. Roberts¹, Gareth Johnson¹,
Katriona Edlmann², Stephanie Flude³ and Zoe K. Shipton¹

¹Department of Civil and Environmental Engineering, University of Strathclyde, Glasgow, UK

²School of Geosciences, University of Edinburgh, Edinburgh, UK

³Department of Earth Sciences, University of Oxford, Oxford, UK

 CJM, 0000-0003-4506-3833

*Correspondence: christopher.mcmahon@strath.ac.uk

Abstract: Engineered geological porous media hydrogen storage must be designed to ensure secure storage, and use appropriate monitoring, measurement and verification tools. Here, we identify and characterize 60 natural hydrogen seeps as analogues for potential leakage from engineered storage reservoirs to consider implications for monitoring. We report and compare the geological and environmental setting; seepage mode (dry gas/associated with water); co-released gases; seep rates and areal fluxes; temporal variation; seep structure; gas source; and composition. Seep characteristics are determined by local geological and hydrological conditions, specifically whether hydrogen gas is seeping through soils and unconsolidated sediments, fractured bedrock or into water. Hydrogen is typically co-emitted with other gases (CO₂, CH₄, N₂) with CH₄, the most common co-emitted gas. The structural controls on seep location and characteristics are similar between hydrogen and CO₂ seeps. However, compared to CO₂, hydrogen is more readily dispersed when mixing with air and hydrogen is more prone to being consumed or transformed via biotic or abiotic reactions, and so the quantity of leaked hydrogen can be greatly attenuated before seeping. Monitoring approaches should therefore be tailored to the local geology and hydrological conditions, and monitoring approaches to detect hydrogen and associated gases would be appropriate.

Supplementary material: Data tables included as supplementary material are available at <https://doi.org/10.6084/m9.figshare.c.6150485>

Hydrogen is proposed to aid the diversification and decarbonization of multiple energy sectors, including heat, transport, power and industry (Hanley *et al.* 2018; Lazarou *et al.* 2018) and provide energy storage to support the expansion of renewable energy. A hydrogen economy could require large-scale hydrogen storage (Heinemann *et al.* 2021), and it is estimated that geological storage of hydrogen could provide gigawatts (GW) of stored energy capacity (IEA 2013; Mouli-Castillo *et al.* 2021). Options for geological hydrogen storage include salt caverns, or porous rocks such as saline aquifers or depleted hydrocarbon reservoirs (Tarkowski 2019), situated onshore or offshore (Heinemann *et al.* 2018; Mouli-Castillo *et al.* 2021). Currently, hydrogen is stored in onshore salt caverns as feedstock for petrochemical processes, with examples in Teesside (UK) and Texas (USA) (Panfilov 2016). To date there has been no industrial storage of 100% hydrogen in porous rock, but some experience was gained during the commercial storage of ‘town gas’ containing *c.* 50% hydrogen in saline

aquifers in France, Germany and the Czech Republic during the 1960s and 1970s (Carden and Paterson 1979).

Engineered geological hydrogen stores must ensure safe and secure storage (Heinemann *et al.* 2021). Leakage from engineered hydrogen stores could have a cascade of environmental, social and economic risks (Heinemann *et al.* 2021; Stalker *et al.* 2022). Understanding how hydrogen might leak out of the geological store, and potentially to the surface, is fundamental to constrain risk in any future geological storage sites. Potential geofluid leakage pathways from the subsurface to the surface have been well documented by decades of research to understand hydrocarbon retention and migration and to ensure containment for the geological storage of CO₂ and radioactive waste. However, differences in the physicochemical properties of hydrogen, and the selection and cyclic operation of storage sites, bring unique scientific challenges (Heinemann *et al.* 2021).

Growing interest in prospecting for natural hydrogen accumulations has led to the identification

From: Miodic, J. M., Heinemann, N., Edlmann, K., Alcalde, J. and Schultz, R. A. (eds) *Enabling Secure Subsurface Storage in Future Energy Systems*. Geological Society, London, Special Publications, **528**, <https://doi.org/10.1144/SP528-2022-59>

© 2023 The Author(s). This is an Open Access article distributed under the terms of the Creative Commons Attribution License (<http://creativecommons.org/licenses/by/4.0/>). Published by The Geological Society of London.

Publishing disclaimer: www.geolsoc.org.uk/pub_ethics

of several surface occurrences of gas that contain native/molecular hydrogen (H_2) (Prinzhofer *et al.* 2018; Vacquand *et al.* 2018; Cathles and Prinzhofer 2020; Zgonnik 2020). Over 300 occurrences of natural hydrogen are documented worldwide (Zgonnik 2020), some of which are interpreted as seeps of a hydrogen-bearing gas that is leaking from a reservoir at depth. Sites of CO_2 and CH_4 seepage have previously provided useful insights for the engineered geological storage of gases in the subsurface, particularly for evaluating measuring, monitoring and verification (MMV) methods. Native hydrogen is physically different to CO_2 and CH_4 , being a small molecule, with a lower density, making it mobile and buoyant. It is highly flammable, but overall, not highly reactive, and has a low solubility in water, meaning it often concentrates in the gas phase. The atmospheric concentration of hydrogen is 0.000531 vol% (Novelli *et al.* 1999), or 0.531 ppm, lower than both CO_2 and CH_4 . The low atmospheric concentration of hydrogen enables relatively easy detection of hydrogen seeps in amounts over this value. These different physico-chemical properties mean hydrogen seeps may be different to CO_2 and CH_4 seeps, and it is important to know what these differences are and, consequently, how MMV for engineered geological hydrogen storage may need to be adapted accordingly. In this paper, we examine a global inventory of hydrogen seepage sites to understand the factors that control their location and characteristics (surface expression, seep rate), leakage mechanisms and implications for the monitoring of geologically engineered hydrogen stores.

Overview of natural hydrogen production, migration, accumulation and consumption in the subsurface

Abiotic and biotic subsurface hydrogen generation and consumption mechanisms are well understood (Sherwood Lollar *et al.* 2014; Panfilov 2016; Gregory *et al.* 2019). Hydrogen is naturally produced in the geological subsurface abiotically through various water–rock interactions and via radiolysis of water during naturally occurring radioactive decay in rocks (Sherwood Lollar *et al.* 2014). Shallow biotic sources of hydrogen include microbes found in soil and as part of insect microbiomes (Conrad and Seiler 1980; Zimmerman *et al.* 1982; Sugimoto *et al.* 1998).

Factors that influence hydrogen flux between source or reservoir and surface include biological activity, temperature, atmospheric pressure, Earth tides and seismic activity (Sugisaki *et al.* 1983; Sato *et al.* 1986; Voitov *et al.* 1995; Cathles and Prinzhofer 2020; Zgonnik 2020), like natural CO_2

seeps (Miocic *et al.* 2016; Roberts *et al.* 2019). However, for hydrogen no studies have yet shown the link between deeper hydrogen reservoirs and surface hydrogen seepage sites.

While conventional oil and gas knowledge may indicate that deep, geologically produced hydrogen is too small and mobile to form economic accumulations, the presence of hydrogen-bearing seeps implies that subsurface accumulations of hydrogen do indeed exist, and significant concentrations of hydrogen have been discovered in a small number of gas reservoirs (Coveney *et al.* 1987; Prinzhofer *et al.* 2018).

In the subsurface, hydrogen may be consumed by methanogen microorganisms to produce organic molecules, the most common being CH_4 . Such biological conversion of hydrogen to CH_4 has been observed in both subsurface ‘town gas’ storage sites (Buzek *et al.* 1994) and in deep mines where drilling introduces microbes that convert geologically produced hydrogen into methane (Warr *et al.* 2021). Hydrogen may also be consumed during abiotic polymerization reactions to produce methane and higher alkanes via processes such as Fischer–Tropsch type reactions (Etiope and Sherwood Lollar 2013). Temporally these reaction rates will vary, with microbial consumption of hydrogen likely to be faster compared to larger-scale geological process reactions.

Methods

First, we expand the Zgonnik (2020) global dataset ($n = 333$) to include newly identified hydrogen seeps ($n = 4$) that have information published since Zgonnik (2020), and prior to February 2022. For the purpose of this study, we refer to all of these published sites as seeps, regardless of whether the original studies convincingly rule out shallow or surface sources of hydrogen (artificial or biotic). We consider sites of seepage to be either surface vents (where gases escape to the atmosphere, e.g. via rock fractures), high concentrations of hydrogen in shallow subsurface boreholes (c. 1 m in soil/rock) and where hydrogen seeps through water as bubbles at the water surface. We then filter the dataset to identify hydrogen seeps that fit two criteria:

- (1) Geological and physical environment: we select seeps that are in geological and physical environments representative of environments analogous to engineered geological hydrogen storage in porous media (e.g. saline aquifers or depleted oil/gas reservoirs) or that show key hydrogen seep processes (e.g. in ophiolites). Thus, we do not consider hydrogen occurrences or seeps associated with mid-ocean ridge zones, gases associated with

drilling of super-deep wells, drilling muds and mining, volcanic gases, high temperature geothermal systems and hydrogen gas in microscopic fluid inclusions or absorbed on mineral surfaces in various rock types and geological settings.

- (2) Source: We do not consider occurrences of hydrogen that are generated by geochemical or biological processes at surface or in the shallow subsurface (e.g. in soil).

Thus, we consider only the 60 out of the total 337 seeps that are analogous to potential engineered hydrogen storage in porous media. For hydrogen seeps that meet these conditions we draw on published information to determine: the geological and environmental setting; whether seepage is as a dry gas or dissolved; co-released gases; seep rates (rate of emission) and fluxes (rate of emission per unit area) and how these were measured or derived; duration of seepage and temporal variation; physical aspects such as the area and shape of seepage; concentration and source of hydrogen. Seeps are numbered (#) and are referred to by the assigned number throughout.

We harmonize units, and report hydrogen concentrations as a percentage (vol%) of relative gas composition. We report seep rate in g(hydrogen)/day, like Roberts *et al.* (2018) and Roberts and Stalker (2020), who report data on CO₂ flux from natural CO₂ seepage sites, field experiments and industry in g m⁻²/day. When converting from m³/day, we take hydrogen density to be 0.0827 kg m⁻³ equivalent to standard temperature (0°C) and pressure (100 kPa).

Where seep rates and/or fluxes are not explicitly reported, we derive these, where possible, from available information. For example, if the area of seepage is reported or can be derived from dimensions or images, and the seep rate is known, gas flux can be calculated. For these calculations, where seep rate is reported as a range, we use the median value to derive the flux (flux = seep rate/area).

Results

Our screening results in 60 seeps in 13 geographical clusters (Fig. 1). Summary information about each seep is detailed in Tables 1–4, with further detail in the supplementary information.

Surface expression of hydrogen seeps

The surface expression of natural hydrogen emanations can be either ‘dry’ ($n = 33$), where hydrogen seeps to atmosphere from rock or soil, or ‘wet’ ($n = 27$), where hydrogen-bearing gases bubble through

water. Wet seeps include those on land associated with rivers and springs ($n = 26$) or on the seabed in the near offshore (continental shelf) ($n = 1$).

The surface expression of dry seeps is governed by outcropping geology and sedimentary cover. Where there is soil or unconsolidated sediments (e.g. sand) hydrogen seeps form circular/subcircular features that are visually prominent ($n = 18$). In contrast, where bedrock crops out, hydrogen seeps form no physical expression, and are spatially constrained, typically to a fracture or several fractures ($n = 14$).

Dry seepage through soils and unconsolidated sediments. We report 19 hydrogen seeps through soils and unconsolidated sediments. 18 sites are circular or oval-shaped features located in five regions; USA (#8–12), Brazil (#14–15), Russia (#1–7), Mali (#13) and Australia (#16–18) (Table 1). These typically manifest as depressions, with changes in vegetation or vegetation loss, and in some cases water collects in them to form permanent or ephemeral lakes. These physical features are sometimes referred to as ‘fairy circles’, but as this term is a specific ecological characterization (Getzin *et al.* 2021), we refer to them as subcircular depressions based on their shape and characteristics and caution against using the term ‘fairy circles’. One site (#19) has no detailed data on the physical expression of seepage.

In the 18 cases of subcircular depressions (#1–18), soils and poorly consolidated modern and Quaternary sediments obscure the bedrock geology. In all these cases the bedrock geology comprises sedimentary rock units overlying metamorphic or igneous basement rocks, typically stable intracratonic basin crust that is Archean to Proterozoic in age (Moretti *et al.* 2021b). For one case (#19), soils overlie metamorphic ophiolitic bedrock directly with no sedimentary cover (Yuce *et al.* 2014).

In many cases, these subcircular depressions form clusters of depressions spanning areas that are thousands of square kilometres; 17 of the entries in our database are in such depression-clusters, covering areas of *c.* 1000 km² (Brazil), 3300 km² (Russia) and 15 000 km² (USA). The remaining two (#13 and #19) are reported as individual depressions, but it is clear from satellite images that other structures do exist in the case of #13. Satellite images for location #19 are less clear and show no obvious features. Individual seep shapes can be circular (#1–7, Larin *et al.* 2015), elliptical (#8–10, #12, Zgonnik *et al.* 2015), and irregular (#14–18, Frery *et al.* 2021; Moretti *et al.* 2021b) – therefore we refer to them collectively as subcircular. There is little published information about the shape, area or size of sites of hydrogen seepage in Mali, although the one depression documented by Prinzhofer *et al.* (2018) (#13) is large and oval-shaped, with a diameter of *c.* 1.5 km.

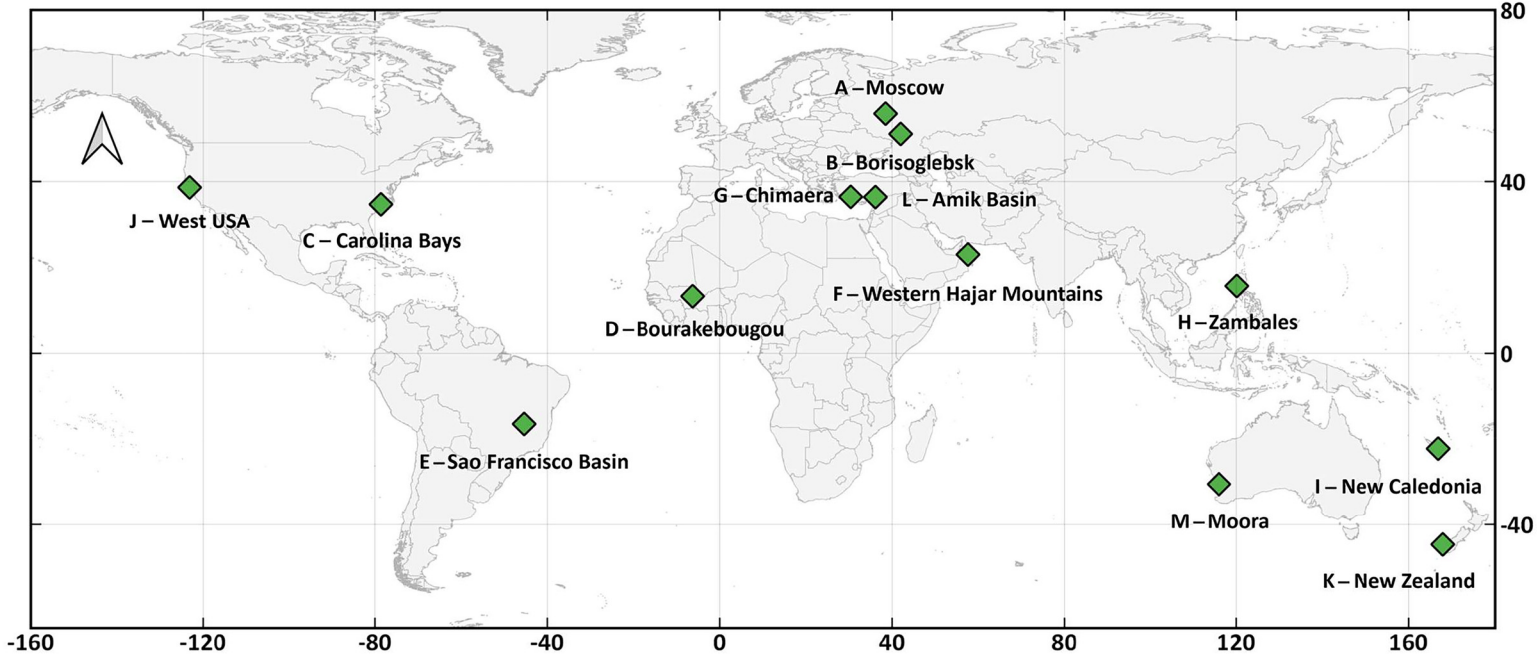


Fig. 1. Location of 60 hydrogen seeps within 13 clusters (letters A–M) that may be analogous of leakage from engineered geological hydrogen stores. The cluster ID (letter – name) is written adjacent and this corresponds to the cluster column in [Tables 1–3](#).

Table 1. Features of natural hydrogen leakage associated with dry seepage through soils and unconsolidated sediments

Seep #	Cluster letter – name	Site/sample name(s)	Location	Lat/long	Geological setting	Exposure/surface geology	Sample method	Gases present	% H ₂	N ₂ %	CH ₄ %	CO ₂ %	O ₂ %	Key reference(s)
1	A – Moscow	Elektrostal	South Moscow, SW Russia	55.773287, 38.50822	Continental platform	Unconsolidated granular sediments	Soil gas (in field)	H ₂ , N ₂ , CH ₄ , CO ₂ , O ₂	0.013	NR	NR	NR	NR	Larin <i>et al.</i> (2015)
2	B – Borisoglebsk	South Oktyabr'skoe	South Moscow, SW Russia	51.052383, 41.998733	Continental platform	Unconsolidated granular sediments	Soil gas (in field)	H ₂ , N ₂ , CH ₄ , CO ₂ , O ₂	0.03–0.055	78.74–78.86	0.0011–0.0013	0.10–0.11	21.03–21.13	
3	A – Moscow	Yakhroma	South Moscow, SW Russia	56.287806, 37.526889	Continental platform	Unconsolidated granular sediments	Soil gas (in field)	H ₂ , N ₂ , CH ₄ , CO ₂ , O ₂	0.0239–0.0508	77.9–78.9	NR	0.3–0.4	21.2–21.7	
4	B – Moscow	Nikulino	South Moscow, SW Russia	56.227124, 37.703246	Continental platform	Unconsolidated granular sediments	Soil gas (in field)	H ₂ , N ₂ , CH ₄ , CO ₂ , O ₂	0.039	78.3	NR	0.7	20.9	
5	B – Borisoglebsk	Ozero Podovoye	South Moscow, SW Russia	51.2298, 42.0362	Continental platform	Unconsolidated granular sediments	Soil gas (in field)	H ₂ , N ₂ , CH ₄ , CO ₂ , O ₂	0.0006–0.2	78.77–79.00	0.0010–0.0014	0.09–0.38	20.52–21.15	
6	B – Borisoglebsk	Satellite Podovoye	South Moscow, SW Russia	51.229867, 43.03516	Continental platform	Unconsolidated granular sediments	Soil gas (in field)	H ₂ , N ₂ , CH ₄ , CO ₂ , O ₂	0.0005–0.3	78.86–79.07	0.0008–0.0013	0.07–0.20	20.72–20.99	
7	B – Moscow	Verevskoye	South Moscow, SW Russia	56.064017, 37.267633	Continental platform	Unconsolidated granular sediments	Soil gas (in field)	H ₂ , N ₂ , CH ₄ , CO ₂ , O ₂	0.1–0.8	78.63–79.37	0.0009–0.0020			
8	C – Carolina Bays	Arthur Road Bay	Carolina Bays, USA	34.7915, –79.2268	Coastal plain	Unconsolidated lacustrine sediments	Soil gas (in field)	H ₂ , N ₂ , CH ₄ , CO ₂ , O ₂	0.0586	79.3	0.0011	0.62	20.05	Zgonnik <i>et al.</i> (2015)
9	C – Carolina Bays	Smith Bay	Carolina Bays, USA	34.6791, –78.5818	Coastal plain	Unconsolidated lacustrine sediments	Soil gas (in field)	H ₂ , N ₂ , CH ₄ , CO ₂ , O ₂	0.0574–0.0715	79.15–79.40	0.0011–0.0017	0.20–0.51	20.23–20.38	
10	C – Carolina Bays	Jones Lake Bay	Carolina Bays, USA	34.682, –78.5963	Coastal plain	Unconsolidated lacustrine sediments	Soil gas (in field)	H ₂ , N ₂ , CH ₄ , CO ₂ , O ₂	0.021–0.0815	NR	NR	NR	NR	
11	C – Carolina Bays	Arthur Road Sandpit	Carolina Bays, USA	34.7871, –79.2267	Coastal plain	Unconsolidated lacustrine sediments	Soil gas (in field)	H ₂ , N ₂ , CH ₄ , CO ₂ , O ₂	0.11	79.28	0.0735	1.21	19.37	
12	C – Carolina Bays	Jones Lake (Smaller Structure)	Carolina Bays, USA	34.693, –78.6005	Coastal plain	Unconsolidated lacustrine sediments	Soil gas (in field)	H ₂ , N ₂ , CH ₄ , CO ₂ , O ₂	0.0719–0.37	78.11–79.61	0.0194–2.7468	0.23–1.38	16.51–20.12	
13	D – Bourakebouyou	Gassola	Gassola, Mali	13.194605, –6.242527	Sedimentary basin	Unspecified soils/sediments	Soil gas (in field)	H ₂ , N ₂ , CH ₄ , CO ₂ , O ₂ + Hydrocarbon Traces	0.001–0.06	NR	NR	NR	NR	Prinzhofer <i>et al.</i> (2018)

(Continued)

Table 1. Continued.

Seep #	Cluster letter – name	Site/sample name(s)	Location	Lat/long	Geological setting	Exposure/surface geology	Sample method	Gases present	% H ₂	N ₂ %	CH ₄ %	CO ₂ %	O ₂ %	Key reference(s)
14	E – Sao Francisco Basin	Campinas	São Francisco Basin, Brazil	–16.560083, –45.343667	Sedimentary basin	Unspecified soils/sediments	Soil gas (in field)	H ₂	0.0221–0.0541	NR	NR	NR	NR	Prinzhofer <i>et al.</i> (2019)
15	E – Sao Francisco Basin	Baru	São Francisco Basin, Brazil	–16.560083, –45.343667	Sedimentary basin	Unspecified soils/sediments	Soil gas (in field)	H ₂	0.001–1.2	NR	NR	NR	NR	Moretti <i>et al.</i> (2021a)
16	M – Moora	Moora: M1, M2, M3, M4, M5	North Perth Basin, Australia	–30.564825, 115.9626	Sedimentary basin	Sediments	Soil gas (in field)	H ₂ , CH ₄ , CO ₂ , O ₂	0–0.0096	NR	0–0.5	0–0.3	20.1–21.7	Frery <i>et al.</i> (2021)
17	M – Moora	Namban: N1	North Perth Basin, Australia	–30.371, 115.984	Sedimentary basin	Sediments	Soil gas (in field)	H ₂ , CH ₄ , CO ₂ , O ₂	0.0005–0.0006	NR	0.2	0.1	21.6–21.7	Frery <i>et al.</i> (2021)
18	M – Moora	Yallalie: Y1, Y2, Y3	North Perth Basin, Australia	–30.467, 115.7765	Sedimentary basin	Sediments	Soil gas (in field)	H ₂ , CH ₄ , CO ₂ , O ₂	0–0.0004	NR	0.1–0.2	0–0.1	20.6–21.9	Frery <i>et al.</i> (2021)
19	L – Amik Basin	Kurtbagi	Turkey	36.4018, 36.0416	Ophiolite	Soil	Soil gas (in field)	H ₂	38.4	NR	NR	NR	NR	Yuce <i>et al.</i> (2014)

All measurements of hydrogen concentration (ppm) are taken in the field using soil gas samples. SAT, sensor saturated; detection limit (of 1100 ppm) reached; NR, not reported.

Table 2. Dry hydrogen seeps not associated with subcircular depression features

Seep #	Cluster number – name	Site/sample name(s)	Location	Lat/long	Geological setting	Exposure/ surface geology	Sample method	Gases present	% H ₂	N ₂ %	CH ₄ %	CO ₂ %	O ₂ %	Key reference(s)
20	F – Western Hajar Mountains	S 1 f 2 (1), S 1 f2 (2)	Oman	23.61986111, 57.11344444	Ophiolitic massif	Gabbro	Borehole gas samples (vacutainers)	H ₂ , N ₂ , CH ₄ , CO ₂	0.008–0.0425	NR	0.0081–0.0082	0	NR	Zgonnik <i>et al.</i> (2019)
21	F – Western Hajar Mountains	S 30 f 1, S 30 f 2	Oman	23.42416667, 57.67205556	Ophiolitic massif	Ophiolitic (e.g. peridotites)	Borehole gas samples (vacutainers)	H ₂ , N ₂ , CH ₄ , CO ₂	0.002–0.0110	NR	0.0024–0.0029	0.0038–0.0058	NR	
22	F – Western Hajar Mountains	S 46 f 1a, S 46 f 1b	Oman	23.39641667, 57.38097222	Ophiolitic massif	Jasper and carbonates	Borehole gas samples (vacutainers)	H ₂ , N ₂ , CH ₄ , CO ₂	0.01–0.0225	NR	0.0011–0.0012	0.0080–0.0116	NR	
23	F – Western Hajar Mountains	S 48 f 1	Oman	23.39633333, 57.38141667	Ophiolitic massif	Jasper and carbonates	Borehole gas samples (vacutainers)	H ₂ , N ₂ , CH ₄ , CO ₂	0.0065	NR	0.0012	0.0115	NR	
24	F – Western Hajar Mountains	S 49 f 2	Oman	23.27425, 57.45791667	Ophiolitic massif	Shales	Borehole gas samples (vacutainers)	H ₂ , N ₂ , CH ₄ , CO ₂	0.045	NR	0.0049	0.0219	NR	
25	F – Western Hajar Mountains	S 50 f 1	Oman	23.27391667, 57.45830556	Ophiolitic massif	Shales	Borehole gas samples (vacutainers)	H ₂ , N ₂ , CH ₄ , CO ₂	0.0625	NR	0	0.0075	NR	
26	F – Western Hajar Mountains	S 51 f 1, S 51 f 2	Oman	23.24105556, 57.42019444	Ophiolitic massif	Marbles	Borehole gas samples (vacutainers)	H ₂ , N ₂ , CH ₄ , CO ₂	0.002–0.0240	NR	0.0015–0.0029	0.0081–0.0102	NR	
27	F – Western Hajar Mountains	S 52 f 2	Oman	23.21208333, 57.39591667	Ophiolitic massif	Shales	Borehole gas samples (vacutainers)	H ₂ , N ₂ , CH ₄ , CO ₂	0.0052	NR	0.0014	0.0202	NR	
28	F – Western Hajar Mountains	S 54 f 1, S 54 f 2, S 54 f 4	Oman	23.2110278, 57.3839722	Ophiolitic massif	Shales	Borehole gas samples (vacutainers)	H ₂ , N ₂ , CH ₄ , CO ₂	0.003–0.3400	NR	0–0.0036	0.0075–0.0088	NR	
29	F – Western Hajar Mountains	S 55 f 1,	Oman	23.17580556, 57.41466667	Ophiolitic massif	Shales	Borehole gas samples (vacutainers)	H ₂ , N ₂ , CH ₄ , CO ₂	0.003–0.04	NR	0.0088	0.0154	NR	
30	F – Western Hajar Mountains	S 61 f 1	Oman	22.882, 57.71163889	Ophiolitic massif	Jasper and carbonates	Borehole gas samples (vacutainers)	H ₂ , N ₂ , CH ₄ , CO ₂	0.006–0.0375	NR	0.0027	0.0167	NR	
31	G – Chimaera	K01, K02, K03, K05, K03, K06	Chimaera, Turkey	36.4314*, 30.4560*	Ophiolitic massif	Ophiolitic	Pyrex bottles (sealed with vacuum stop-cocks)	H ₂ , N ₂ , CH ₄ , CO ₂	7.46–11.3	2.1–4.9	86.5–87.78	0.01–0.07	NR	Hosgörmez <i>et al.</i> (2008)
32	H – Zambales	LFE-3, LFE-3	Zambales, Philippines	15.5718, 120.1513	Ophiolitic massif	Ophiolitic	Evacuated stainless steel containers	H ₂ , N ₂ , CH ₄ , CO ₂ , O ₂	42.3–42.6	1.5–1.8	54.8–55.3	<0.01–0.03	NR	Abrajano <i>et al.</i> (1988)
33	H – Zambales	Nagasa	Zambales, Philippines	14.837, 120.1282	Ophiolitic massif	Ophiolitic	Stainless steel tubes (w/ helium proof valves)	H ₂ , CH ₄ , CO ₂	58.5	1.2	Not reported	<0.01	NR	Vacquand <i>et al.</i> (2018)

NR, not reported.

Table 3. *Hydrogen seeps where the emission style is as reduced gas seepages associated with bubbling waters*

Seep #	Cluster number – name	Site/sample name	Location	Lat/long	Geological setting	Exposure/ surface geology	Surface expression	Sample method	Gases present	% H ₂	N ₂ %	CH ₄ %	CO ₂ %	O ₂ %	Key reference(s)
34	I – New Caledonia	Carénage 1, Carénage 2	New Caledonia	–22.3048, 166.8409	Ophiolitic massif	Ophiolitic (e.g. peridotites)	Springs	Vacutainer	H ₂ , N ₂ , CH ₄ , CO ₂	32.4–36.07	50.25–51.86	13.68–15.74	0	NR	Deville and Prinzhofer (2016), Vacquand <i>et al.</i> (2018)
35	I – New Caledonia	Kaoris 1, Kaoris 2, Kaoris 3	New Caledonia	–22.2994, 166.8618	Ophiolitic massif	Ophiolitic (e.g. peridotites)	Springs	Vacutainer	H ₂ , N ₂ , CH ₄ , CO ₂	26.81	55.29–61.9	11.26–11.54	0	NR	
36	F – Western Hajar Mountains	Magniyat	Oman	23.4061, 56.8633	Ophiolitic massif	Ophiolitic (e.g. peridotites)	Springs	Stainless steel tubes (w/ helium proof valves)	H ₂ , N ₂ , CH ₄ , CO ₂	87.3	9.8	2.9	0.01	NR	Vacquand <i>et al.</i> (2018)
37	F – Western Hajar Mountains	Hawasina	Oman	23.6833, 56.9396	Ophiolitic massif	Ophiolitic (e.g. peridotites)	Springs	Stainless steel tubes (w/ helium proof valves)	H ₂ , N ₂ , CH ₄ , CO ₂	85.9	9.4	4.6	0.01	NR	
38	F – Western Hajar Mountains	Bahla (2008, 2012)	Oman	22.9922, 57.2932	Ophiolitic massif	Ophiolitic (e.g. peridotites)	Springs	Stainless steel tubes (w/ helium proof valves)	H ₂ , N ₂ , CH ₄ , CO ₂	85.7	12–12.4	1.9–2.2	0.01	NR	
39	F – Western Hajar Mountains	Kufeis	Oman	23.9588, 56.44	Ophiolitic massif	Ophiolitic (e.g. peridotites)	Springs	Stainless steel tubes (w/ helium proof valves)	H ₂ , N ₂ , CH ₄ , CO ₂	85.4	14.5	0.1	0.01	NR	
40	F – Western Hajar Mountains	Haylan (2010, 2021-2a, 2012-6, 2021-8)	Oman	23.6199, 57.1132	Ophiolitic massif	Ophiolitic (e.g. peridotites)	Springs	Stainless steel tubes (w/ helium proof valves)	H ₂ , N ₂ , CH ₄ , CO ₂	75–79.4	14.2–18.1	4–9.6	0.01	NR	
41	F – Western Hajar Mountains	Barrage (Jizzi)	Oman	24.3282, 56.1307	Ophiolitic massif	Ophiolitic (e.g. peridotites)	Springs	Stainless steel tubes (w/ helium proof valves)	H ₂ , N ₂ , CH ₄ , CO ₂	75.2	14.9	10	0.01	NR	
42	F – Western Hajar Mountains	Halhal	Oman	23.7172, 57.034	Ophiolitic massif	Ophiolitic (e.g. peridotites)	Springs	Stainless steel tubes (w/ helium proof valves)	H ₂ , N ₂ , CH ₄ , CO ₂	73.4	20.8	5.8	0.01	NR	

(Continued)

Table 3. Continued.

Seep #	Cluster number – name	Site/sample name	Location	Lat/long	Geological setting	Exposure/ surface geology	Surface expression	Sample method	Gases present	% H ₂	N ₂ %	CH ₄ %	CO ₂ %	O ₂ %	Key reference(s)
43	F – Western Hajar Mountains	Alkar	Oman	23.9693, 56.4219	Ophiolitic massif	Ophiolitic (e.g. peridotites)	Springs	Stainless steel tubes (w/ helium proof valves)	H ₂ , N ₂ , CH ₄ , CO ₂	68.1	28.5	3.3	0.01	NR	
44	F – Western Hajar Mountains	Huqain	Oman	23.5352, 57.3333	Ophiolitic massif	Ophiolitic (e.g. peridotites)	Springs	Stainless steel tubes (w/ helium proof valves)	H ₂ , N ₂ , CH ₄ , CO ₂	65.1	32.4	2.5	0.01	NR	
45	F – Western Hajar Mountains	Lauriers Roses	Oman	22.8956, 58.3946	Ophiolitic massif	Ophiolitic (e.g. peridotites)	Springs	Stainless steel tubes (w/ helium proof valves)	H ₂ , N ₂ , CH ₄ , CO ₂	61	23.2	15.4	0.01	NR	
46	F – Western Hajar Mountains	Abyiad (2010, 2010-29, 2010-30)	Oman	23.4285, 57.6683	Ophiolitic massif	Ophiolitic (e.g. peridotites)	Springs	Stainless steel tubes (w/ helium proof valves)	H ₂ , N ₂ , CH ₄ , CO ₂	26.9–36.1	57.3–59.9	5.7–15.9	0.01	NR	
47	F – Western Hajar Mountains	Bahla (1, 2, 3, 4, 5)	Oman	22.9922, 57.2932	Ophiolitic massif	Ophiolitic (e.g. peridotites)	Springs	Glass bottles (w/ teflon seals)	H ₂ , N ₂ , O ₂ , CH ₄	43–97	2–43	0.9–2.2	NR	0.1–13	Neal and Stanger (1983)
48	F – Western Hajar Mountains	Hawqayn (1, 2, 3)	Oman	23.5457*, 57.3411*	Ophiolitic massif	Ophiolitic (e.g. peridotites)	Springs	Glass bottles (w/ teflon seals)	H ₂ , N ₂ , O ₂ , CH ₄	39–48	39–50	1.1–4.3	NR	8–10	
49	F – Western Hajar Mountains	Nizwa	Oman	22.9373*, 57.3335*	Ophiolitic massif	Ophiolitic (e.g. peridotites)	Springs	Glass bottles (w/ teflon seals)	H ₂ , N ₂ , CH ₄	95	1	4	NR	0	
50	F – Western Hajar Mountains	Huwayl Qufays	Oman	23.9566, 56.4371*	Ophiolitic massif	Ophiolitic (e.g. peridotites)	Springs	Glass bottles (w/ teflon seals)	H ₂ , N ₂ , CH ₄	99	1	0	NR	0	
51	F – Western Hajar Mountains	B'lad	Oman	24.25*, 56.12*	Ophiolitic massif	Ophiolitic (e.g. peridotites)	Springs	Glass bottles (w/ teflon seals)	H ₂ , N ₂ , O ₂ , CH ₄	22	76	0	NR	1	
52	F – Western Hajar Mountains	S 30 (1), S 30 (2)	Oman	23.42416667, 57.67205556	Ophiolitic massif	Ophiolitic (e.g. peridotites)	Bubbling springs	Glass bell and flow chamber	H ₂ , N ₂ , O ₂ , CH ₄ , CO ₂	30.3–30.7	60.6–61	7.5–7.6	0	1.1	Zgonnik <i>et al.</i> (2019)
53	F – Western Hajar Mountains	S 8 (1), S 8 (2)	Oman	23.61805556, 57.10780556	Ophiolitic massif	Ophiolitic (e.g. peridotites)	Bubbling springs	Glass bell and flow chamber	H ₂ , N ₂ , O ₂ , CH ₄ , CO ₂	70–71.7	23–24.3	3.5	0	1.7–2.2	
54	F – Western Hajar Mountains	S 39 (1), S 39 (2)	Oman	23.42933333, 57.66825	Ophiolitic massif	Terraces	Bubbling springs	Glass bell and flow chamber	H ₂ , N ₂ , O ₂ , CH ₄ , CO ₂	35.1–37.3	52.8–54.3	6.2–6.8	0	3.1–4.4	

(Continued)

Table 3. Continued.

Seep #	Cluster number – name	Site/sample name	Location	Lat/long	Geological setting	Exposure/ surface geology	Surface expression	Sample method	Gases present	% H ₂	N ₂ %	CH ₄ %	CO ₂ %	O ₂ %	Key reference(s)
55	F – Western Hajar Mountains	S 2-1	Oman	23.6198889, 57.11319444	Ophiolitic massif	Gabbro	Bubbling springs	Glass bell and flow chamber	H ₂ , N ₂ , O ₂ , CH ₄ , CO ₂	77	14.2	8.8	0	0	
56	J – West USA	Barnes Spring (1, 5, 7), NS1, Camp Spring	Austin Creek, USA	38.6207, -123.1339	Subduction Complex	Peridotite	Bubbling springs	Beaker, then into pre-evacuated serum vials	H ₂ , N ₂ , CH ₄ , CO ₂	15.7–50.9	36.6–63.1	5.3–15.8	0	NR	Morrill <i>et al.</i> (2013)
57	K – New Zealand	Poison Bay	Milford Sound, New Zealand	-44.6718, 167.927	Orogenic	Ultramafic, Mylonitic Gneiss	Bubbling offshore	Not reported	H ₂ , N ₂ , O ₂ , CH ₄ , CO ₂	56.4	20.2	16.6	0.7	6.1	Wood (1972)
58	L – Amik Basin	Tahtakopru	Turkey	36.3835, 36.1636	Ophiolite	Ophiolitic (e.g. peridotites)	Bubbling springs	Inverted funnel	H ₂	60.5	NR	NR	NR	NR	Yuce <i>et al.</i> (2014)
59	H – Zambales	LFE-1	Zambales, Philippines	15.6754*, 120.0827*	Ophiolitic massif	Ophiolitic	Bubbling springs	Evacuated stainless steel containers	H ₂ , N ₂ , O ₂ , CH ₄ , CO ₂	8.4	60.6	13	0.03	16.5	Abrajano <i>et al.</i> (1988)
60	H – Zambales	Mangatarem	Philippines	15.7033, 120.2825	Ophiolitic massif	Ophiolitic (e.g. peridotites)	Springs	Stainless steel tubes (w/ helium proof valves)	H ₂ , N ₂ , CH ₄ , CO ₂	35.1	48	16.7	0.01	NR	Vacquand <i>et al.</i> (2018)

These are all found in ophiolitic settings. In most cases, hydrogen is thought to be as a product of serpentinization processes. * Indicates approximate location where lat/long is not provided in the literature. NR, not reported.

Table 4. *Hydrogen seep rates*

<i>N</i>	Site/sample name	Seep rate (m ³ /day)	Average seep rate (m ³ /day)	Average seep rate (g/day)	Seep diameter (m)	Seep radius (m)	Seep radius (km)	Area (km ²)	Average flux (m ³ /day/km ²)	Average flux (g m ⁻² /day)	Key reference(s)
1	Elektrostal	30–50	40	3308	219	109	0.109	0.0375	800–1335	0.088	Larin <i>et al.</i> (2015)
5	Ozero Podovoye	3750–4800	4275	353 542.5	1000	500	0.500	0.785	575–740	0.450	
6	Satellite Podovoye	40	40	3308	100	50	0.050	0.008	5093	0.421	
7	Verevskoye	21 000–27 000	24 000	1 984 800	1000	500	0.500	0.785	7 000 000–9 000 000	2.527	
8	Arthur Road Bay	1000–1370	1185	97 999.5	782	391	0.391	0.48	2240–3060	0.204	Zgonnik <i>et al.</i> (2015)
9	Smith Bay	750–1000	875	72 362.5	1205	602	0.602	1.14	660–880	0.063	
10	Jones Lake Bay	1120–2740	1930	159 611	2821	1410	1.410	6.25	180–440	0.026	
12	Jones Lake (Smaller Structure)	21–31	26	2150.2	94	47	0.047	0.007	3000–4400	0.307	
14	Capinas	80–102	85	700 000	539	264	0.264	0.22	385	0.32	Moretti <i>et al.</i> (2021a)
15	Baru	51–77	64	530 000	460	230	0.230	0.17	385	0.32	
N/A	Peridotites	13 505–27 195	20 348	1 682 779.6	Not a circle	Not a circle	Not a circle	185	110	0.01	Zgonnik <i>et al.</i> (2019)
N/A	Proterozoic Sediments	29 700–85 800	57 750	4 775 925	Not a circle	Not a circle	Not a circle	66	875	0.072	

N corresponds to numbers in previous tables where applicable and N/A for those that are not site specific, but rather seepage rates over larger geological units.

Subcircular features associated with hydrogen seepage have been observed to appear and establish over short timeframes (1–2 years). For example, time-lapse satellite images track the formation of the Elektrostal seep (#1) over a two-year period between 2002 and 2004 (Larin *et al.* 2015), and the formation of the Jones Lake Bay seep (#10) over a one-year period (Zgonnik *et al.* 2015). In both cases, the onset of feature formation and hydrogen seepage is documented at these sites, and seepage is ongoing (or seep cessation is not yet reported). Subcircular features in the Carolina region have been shown to exist for tens of thousands of years using optically-stimulated luminescence, LiDAR and other data (Moore *et al.* 2016; Piovan and Hodgson 2017). Moretti *et al.* (2021b) found that in agricultural areas in Brazil, archive images show the reappearance of features following disturbance by ploughing; however, they also note that the appearance/disappearance of new structures is often not observed or reported.

A change in vegetation or vegetation loss is often associated with these features (Larin *et al.* 2015; Zgonnik *et al.* 2015; Prinzhofer *et al.* 2019; Frey *et al.* 2021). When depressions have a shallow water table often a lake or wetlands form in the sunken centre as the land subsides. Frey *et al.* (2021) note that new trees have become established on the external ring of two actively seeping depressions in Australia. Furthermore, Frey *et al.* (2021) note that vegetation distribution and disturbance is not uniform between sites in the same location with active hydrogen seepage.

The diameter of subcircular features varies between sites; ranging from tens of metres (#3) to kilometres (#2) (Larin *et al.* 2015; Zgonnik *et al.* 2015). Moretti *et al.* (2021b) found an average diameter of hydrogen seep depressions between 200 and 300 m from the sites they collated from Brazil, Russia and Australia. Larin *et al.* (2015) studied depressions in Russia and Australia (many of them not sampled for hydrogen) and found a sub-exponential relationship between size and frequency for depressions (with a diameter <1000 m); for instance, smaller depressions are more common than larger depressions.

The maximum depth (amplitude) is only explicitly quantified for 4 out of the 18 subcircular depression sites (#5, #8, #9, #14) and ranges from *c.* 1 to 8 m. Two of these seeps (#8 and #9) have an outer raised rim of *c.* 3 m rather than an internal depression. The cross-sectional depth profile is rounded (i.e. plate shaped) rather than cone or bowl shaped (#5, #8, #9, #14).

Hydrogen concentrations are reported for all 19 dry, soil and sediment-hosted seeps (Fig. 2). There are 18 seeps (#1–18) using soil gas sampling methods, and while the measurement depth is not

consistent between studies, from 0.10 to *c.* 1.2 m (Larin *et al.* 2015; Zgonnik *et al.* 2015; Prinzhofer *et al.* 2019), there is no clear correlation between sampling depth and hydrogen concentration. Sampling depths are not reported at seep #13 (Prinzhofer *et al.* 2018). Reported hydrogen concentrations range from 0.0001–99% (Fig. 2).

Soil gas sampling at seeps #1–12 and #16–18 reports hydrogen concentrations that are spatially variable within depressions (Figs 3 & 4), but typically highest nearer the edge (or rim) of larger subcircular depressions (Larin *et al.* 2015; Zgonnik *et al.* 2015; Frey *et al.* 2021; Moretti *et al.* 2021b). These higher concentrations of hydrogen have been observed to correspond with soils or sediments of higher permeabilities (e.g. sand) (Zgonnik *et al.* 2015). Some features in seeps #1–12 have hydrogen emissions outside the subcircular depression (Fig. 4), whereas in seeps #13–14 this is not the case (Moretti *et al.* 2021b). Features that are filled with water have not been measured for hydrogen concentration due to the measurement technique (soil gas sampling) not being suitable.

In seeps #1–13 and #16–18, other gases associated with hydrogen are reported (Fig. 5). While these samples are collected from atmosphere, not soil gas wells, the concentrations of methane and carbon dioxide are above their respective atmospheric levels alongside hydrogen. In seeps #8–12, CH₄ concentrations vary from 0.0011–27.5%; however, in #11, Zgonnik *et al.* (2015) observe gas bubbling in stagnant pools that contains no hydrogen despite its presence in soil gas at the same location. Instead, the gas bubbling from the pools consists of 35% N₂, 53% CH₄ and 9% CO₂ (Zgonnik *et al.* 2015).

Dry seepage from rock fractures. There are 14 cases of hydrogen emitted directly from the bedrock, without overlying soil or sediments. Of these, 3 cases manifest as hydrogen-bearing gas actively venting from bedrock fractures (#31–33) and 11 cases are of high concentrations of hydrogen gas measured *in situ* within subsurface fractures (#20–30) (Table 2). All the fracture seeps (Oman, Turkey and the Philippines) have a common geological setting: ophiolitic or subduction complexes (compression zones). These types of emissions have been referred to in the literature as reduced gas seepages, due to their composition (H₂, CH₄, N₂) and interpreted formation processes (Vacquand *et al.* 2018).

Field measurements of hydrogen concentrations (ppm) are reported for 11 of the 14 sites – all from seeps in Oman (Fig. 6). Concentrations of hydrogen range from 20 to 3400 ppm. Hydrogen is co-released with N₂, CO₂ and CH₄ (Fig. 5) and minor components of other gases (e.g. noble gases and/or hydrocarbons). There is no relationship between the

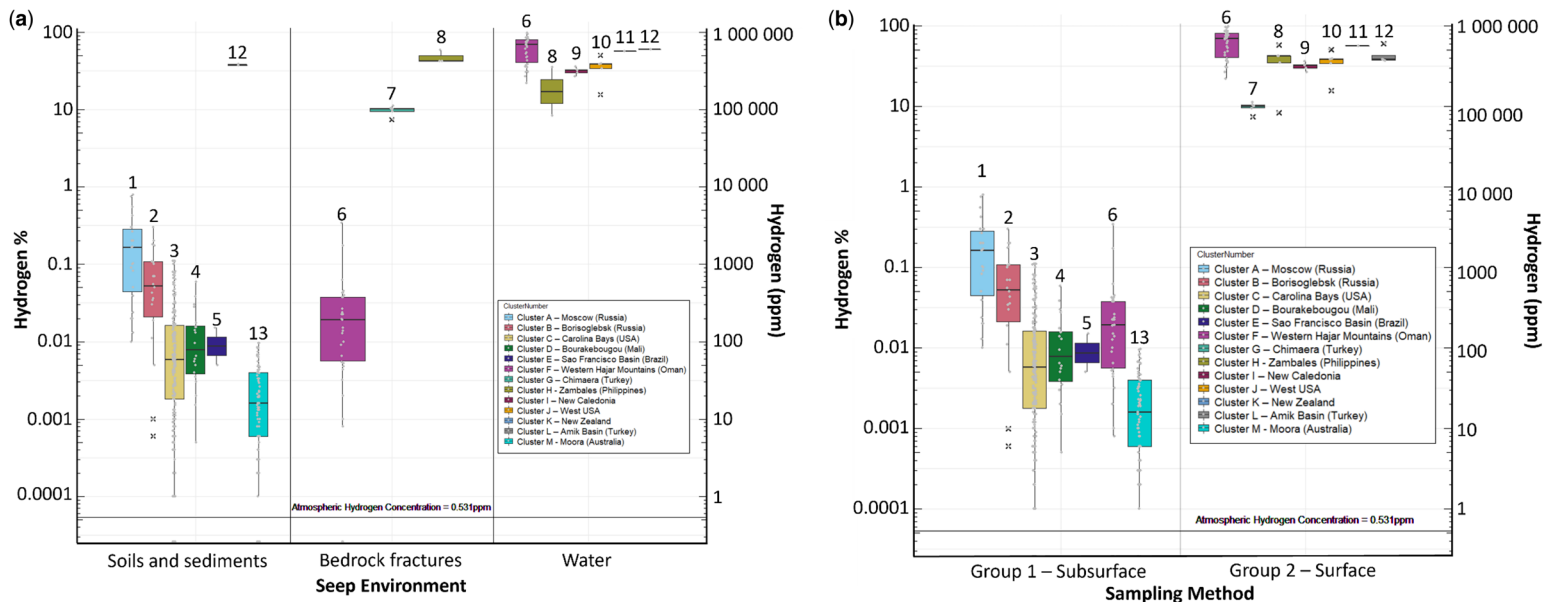


Fig. 2. Hydrogen concentrations (vol%) for each cluster of seepage sites, plotted as **(a)** a function of seep type and **(b)** a function of measurement type (i.e. whether measured in the near surface, top *c.* 1 m in soils/fractured rock (Group 1) or at the surface in gas vents or bubbles (Group 2)). Coloured boxes represent the sample median (horizontal line), and the first and third quartiles, with the extending lines representing the minimum and maximum values. Grey dots show the data points, black crosses show outliers. Numbers on/near boxplots correspond to cluster number in [Tables 1–3](#) and [Figure 1](#). Seep cluster ID F has hydrogen seeping via bedrock fractures and bubbles in water and thus has gas sampled both from the subsurface and the surface.

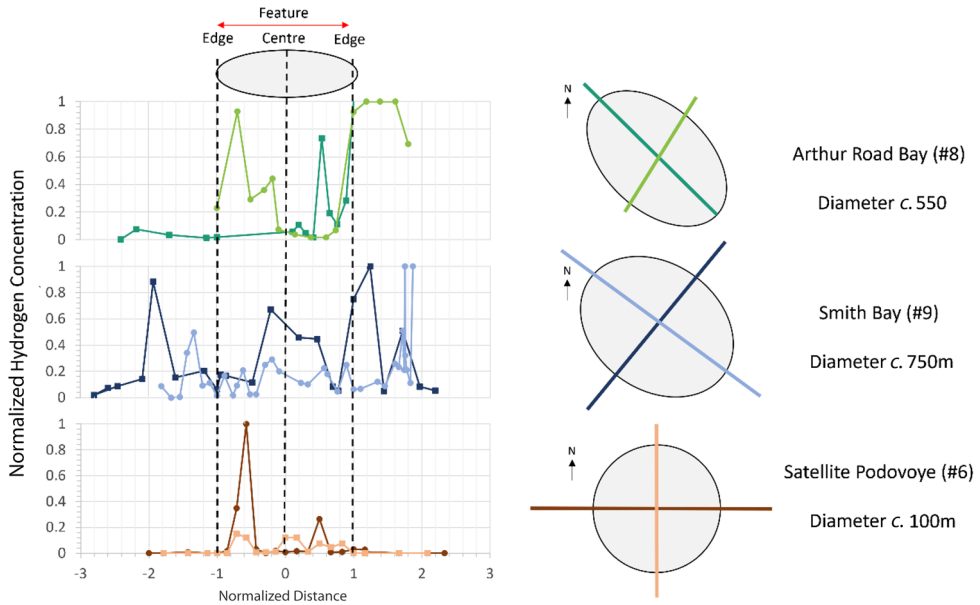


Fig. 3. Soil gas profiles of Smith Bay (#9, *Zgonnik et al. 2015*), Arthur Road Bay (#8, *Zgonnik et al. 2015*) and Satellite Podovoye (#6, *Larin et al. 2015*). Distance on the *x*-axis is normalized so that a value of 1 corresponds to the edge of the depression feature. This allows comparison between features of different sizes. Hydrogen concentrations are normalized where the maximum concentration taken along a transect is = 1. Measurements that were recorded as SAT (= detector saturated) were set to 1. Depression shape, size, orientation and transect orientations are shown for each site.

exposed rock type and the hydrogen concentration for the dry seeps in Oman (*Fig. 6*).

Two of the 14 sites (#31–32, in Turkey and the Philippines) are seeps that are dominantly composed

of CH₄, with subsidiary hydrogen (7–42% H₂). These seeps are famous for long-lived flames which emanate from rock fractures and ignite spontaneously (*Hosgörmez et al. 2008; Vacquand et al.*

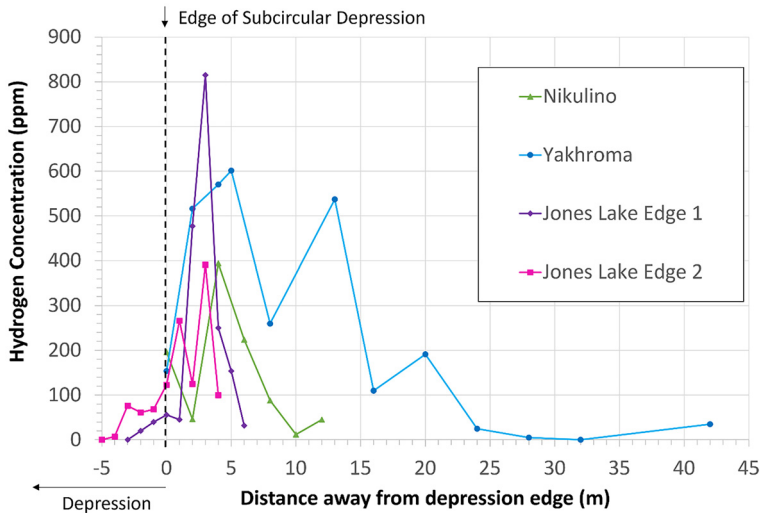


Fig. 4. Transects of hydrogen concentration at the edge of the Nikulino (#4, *Larin et al. 2015*), Yakhroma (#3, *Larin et al. 2015*) and Jones Lake Bay (#10, *Zgonnik et al. 2015*) features.

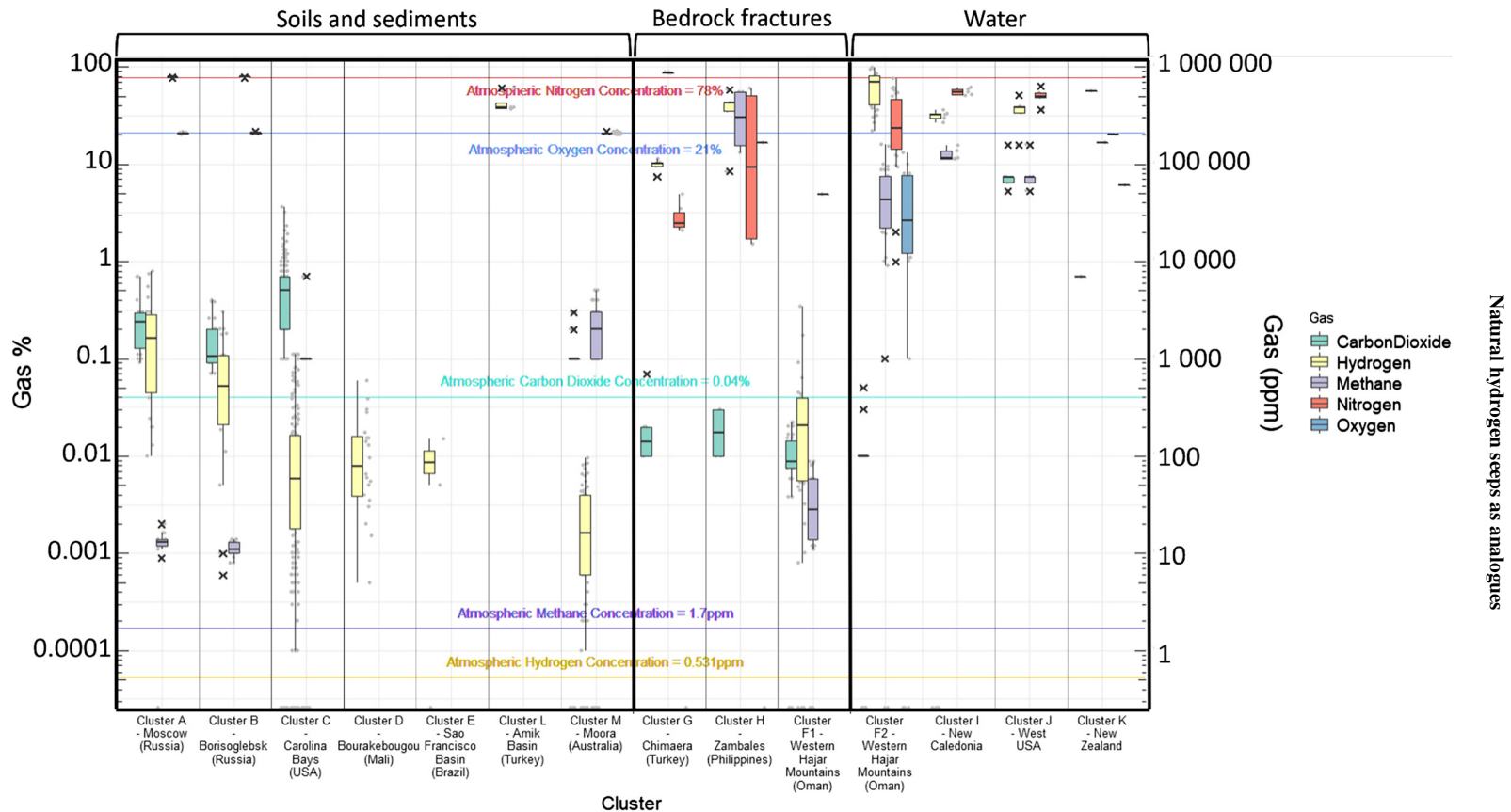


Fig. 5. Measured gas concentrations reported from hydrogen seepage sites. Clusters are organized by surface expression of seepage. Cluster 6 is split into two sections to represent different surface expression of seepage, either via (a) bedrock fractures or (b) water. Coloured boxes represent the sample median (horizontal line), and the first and third quartiles, with the extending lines representing the minimum and maximum values. Grey dots show the data points, black crosses show outliers.

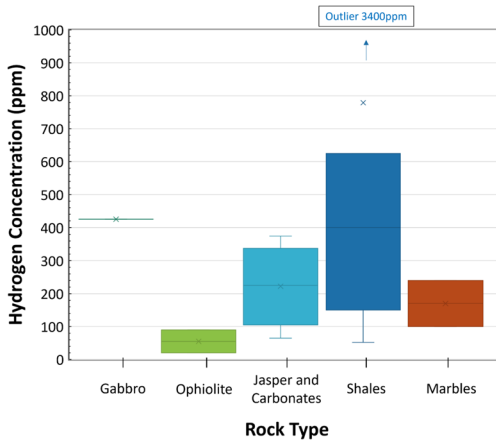


Fig. 6. Hydrogen concentrations (ppm) of seepage from specific rock types in Oman. Coloured boxes represent the sample median (horizontal line), and the first and third quartiles, with the extending lines representing the minimum and maximum values. Crosses indicate outliers. The shale outlier reporting 3400 ppm is seep #28, where the shales directly overlie Precambrian basement and are below the ophiolite nappe.

2018). The Los-Fuegos Eternos seeps (#32, Table 2) have been burning for over 2500 years (Hosgörmez *et al.* 2008).

Wet seepage through water. We found 27 ‘wet’ seeps where hydrogen-bearing gases bubble through water, either on land at springs ($n = 26$) or to seabed in the near offshore (continental shelf) ($n = 1$) (Table 3). These are located in 6 regions: Oman ($n = 20$), New Caledonia ($n = 2$), Philippines ($n = 2$), Turkey ($n = 1$), USA ($n = 1$) and New Zealand (1). Within Oman, the springs form sub-clusters within the Western Hajar mountains.

In all cases, hydrogen is seeping from ophiolitic and subduction-related rocks, such as peridotites. The springs are ultrabasic (hyperalkaline) systems that locally precipitate carbonate (Neal and Stanger 1983; Deville and Prinzhofer 2016; Vacquand *et al.* 2018).

For ‘wet’ hydrogen seeps, hydrogen concentrations vary from 8.4 to 99% of the total gas volume (Fig. 2a). Hydrogen is the major gas at 17 sites (15 of which are in Oman). When hydrogen is a major gas, it comprises 43% or greater and up to 99% (#50), and is commonly associated with CH_4 , N_2 or CO_2 , each typically below 10% (Figs 4 & 5). N_2 is the dominant gas at 9 sites all in New Caledonia or the Philippines, whereas at Bahla, Oman (#38), N_2 and hydrogen are in equal proportion and both dominant. For 12 seeps, there are multiple measurements within the same spring and hydrogen

concentrations can vary considerably between samples (e.g. #47, hydrogen concentration range 43–97%).

Oman is the only cluster of hydrogen seeps that have two distinct types of seepage – both ‘wet’ seeps from springs and ‘dry’ seeps from fractured rock, both of which are in peridotites.

Hydrogen concentration and seep rates

Hydrogen concentrations can be split into two distinct groups (Fig. 2b). Group 1 with concentrations below 1% includes all subcircular depression seeps and all the bedrock fracture seepage sites in Oman. At these sites concentration measurements are collected after creating a borehole in soils or rock. Group 2 with concentrations above *c.* 7–10% includes all seepage through water, plus the bedrock fracture and soil seepage sites in Turkey and the Philippines. These measurements were all collected in containers (from rock fractures or bubbling springs) and then analysed in a lab via gas chromatography.

Hydrogen seep rates are reported in the literature for 10 of the seeps associated with subcircular depression features (Table 4), and for 2 rock units in Oman associated with dry fractured bedrock type seeps. Where a range of seep rates are reported for a site, authors note this is due to uncertainty in the assumptions made in the calculation (e.g. different values for soil porosity (Zgonnik *et al.* 2015), or the area chosen to represent seepage), rather than temporal variability. Where seep rate is reported in the literature, we take an average (median) value of this seepage rate range, and thus the rate has some uncertainty.

Seep rate (Fig. 7) ranges between locations from 0.002 t of hydrogen per day (0.78 t per year, #12 Table 4), through to 2 t per day (700 t per year, #7). There is no relationship between seep rate and spatial location. Seepage sites with larger spatial extent have higher total seep rate, but this could simply reflect the calculation method.

Seep flux (Fig. 8) is reported for 4 seeps (#8–10, 12) and calculated for the remaining 8 seeps. Flux tends to be on the order of 0.002 t of hydrogen per day (0.73 t per year) to 5 t of hydrogen per day (1825 t a^{-1}). Similar to seep rates, we observe no relationship between flux rate and spatial location. Further, there is no relationship between flux and the size of the seep, though there are relatively few data points.

Discussion

Characteristics of hydrogen seepage sites

Whilst the physical and geological environment controls the surface expression of hydrogen seepage,

Natural hydrogen seeps as analogues

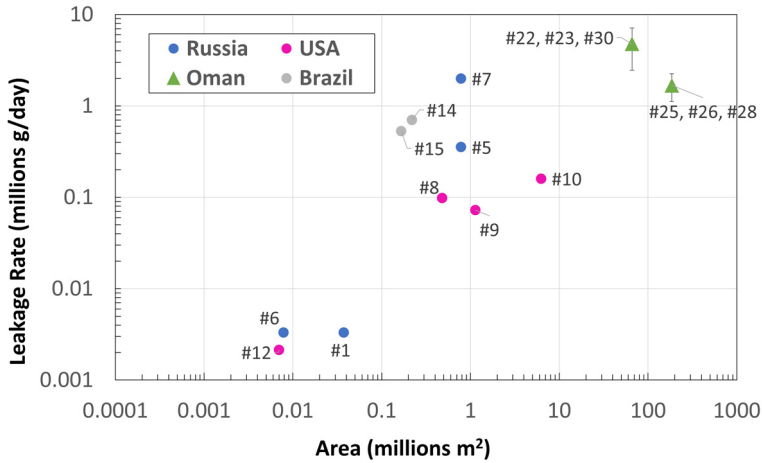


Fig. 7. Seep area v. reported rate of hydrogen seepage. Numbers (#) are seep numbers (Tables 1–4). Markers represent surface expression of seepage: circles represent soils and sediments, and triangles represent bedrock fractures. Error bars represent maximum and minimum leakage rates constrained by uncertainties in assumptions. Seep area is the footprint of the subcircular depression, or the size of the region of leakage. Source: data from Larin *et al.* (2015), Zgonnik *et al.* (2015, 2019) and Moretti *et al.* (2021a).

variability is observed between seep characteristics and rate of emission within similar environments.

Seepage controls on measured hydrogen concentration. We see two distinct groups in the hydrogen concentration data (Fig. 2b). This could be explained as gases bubbling through water are likely to have higher concentrations compared to soil gas as the gas from depth is less diluted by air. Also, when gas bubbles through water, the more soluble co-existing gases will dissolve out faster than hydrogen,

which means hydrogen concentrations in the gas phase will increase. However, more work may be required to ensure that the split in data is not due to sampling artefacts in the data collected as there is a split between those samples collected in shallow boreholes (e.g. soil gas wells, and in fractured rocks to *c.* 1 m depth) (Group 1, <1% hydrogen) and those collected directly from bubbling springs or gas vents (Group 2, >7% hydrogen) (Fig. 2b).

Pulses and daily cycles of seepage are observed at natural hydrogen seeps where seepage occurs

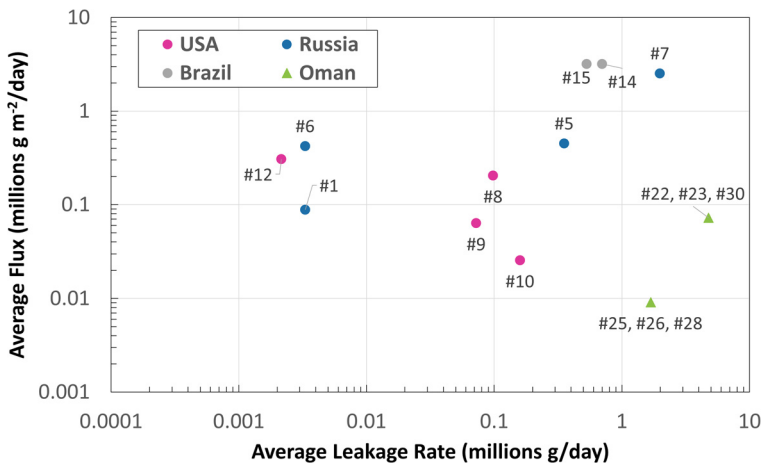


Fig. 8. Flux v. leakage rate. Numbers (#) are seep numbers (Tables 1–4). Markers represent surface expression of seepage: circles represent soils and sediments, and triangles represent bedrock fractures.

through soils and unconsolidated sediments (Prinzhofer *et al.* 2019; Moretti *et al.* 2021a). Continuous monitoring of hydrogen concentrations over 1–8 months at two seeps in Brazil located c. 1.5 km from each other (#14, #15) found that hydrogen emissions varied with time (Prinzhofer *et al.* 2019; Moretti *et al.* 2021a). These studies used sensors spaced tens of metres apart and found two types of temporal variability: daily diurnal cycles and apparently random short-lived increased emission events which cause greater variation. Spatial variability was observed across the depression as sensors recorded different readings of hydrogen concentrations, even during ‘pulse’ events (Moretti *et al.* 2021b). The distribution of concentrations was patchy, including areas of no measurable hydrogen. Further, transects across these features in Russia and the USA (#1–12) indicate that hydrogen seepage is spatially variable, but often higher at or near the depression edge (Figs 3 & 4), indicating localized preferential migration pathways of hydrogen in the near surface. These preferential pathways likely focus in higher permeability soils and sediments (Myagkiy *et al.* 2020b). Moretti *et al.* (2021b) note that even around the rim the emission rates were spatially different. The daily cycle of emissions can be seen across multiple sensors; however, the short-lived increased emission events were limited to specific monitoring locations and did not manifest across the whole seep area. These two studies concluded that the observed spatial variability in hydrogen concentrations indicate that different preferential seepage pathways must exist, influenced by soil characteristics (e.g. permeability) and heterogeneity, and that these pathways can have an effect temporally on when hydrogen reaches the surface from the subsurface source or point of leakage (Moretti *et al.* 2021b). However, neither study effectively ruled out the possibility of a biological or microbial source of the measured hydrogen, and it is possible that the observed spatial and temporal variability represents biological action rather than gas seepage.

Our compilation suggests that where seepage occurs through soils and unconsolidated sediments, the seep rate is roughly proportional to seep area (Fig. 7). However, there are very few data points (seep rate is calculated for only 10 of the 60 identified seeps in this study), and this inferred relationship might be an artefact of the assumptions and uncertainties within seep flux and seep rate calculations. Firstly, flux is very sensitive to estimates of the seep area (Prinzhofer *et al.* 2019). Secondly, flux calculations assumed consistent flux, and did not account for variations with space and time as has been observed at natural hydrogen seeps where seepage occurs through soils and unconsolidated sediments (Prinzhofer *et al.* 2019; Moretti *et al.* 2021a). The calculations also typically do not

account for any diffusive flux around seep hotspots (e.g. Prinzhofer *et al.* 2019; Zgonnik *et al.* 2019). Where emission rates are reported, they are derived by the rate of accumulation into soil gas sampling wells. This methodology uses a pump, resulting in a disturbance of both advective and diffusive gas flow in the soils, meaning that gas emission rates are likely to be over-estimated. Recent models by Myagkiy *et al.* (2020b) do not consider this effect. While measurement of hydrogen fluxes in nature is known to be difficult (Meredith *et al.* 2014), more robust measurement methods and techniques, such as use of closed-system soil gas chambers, should be used to measure hydrogen flux measurements more accurately. Current flux and seepage rate data are therefore problematic and these large uncertainties may explain the lack of relationship between seep rate and flux (Fig. 8). There are currently not enough data to draw comparisons of seep rate and flux between different measured hydrogen concentrations or surface expressions of seepage.

Physical and structural features of hydrogen seeps.

Documented hydrogen seeps are associated with structural and physical manifestations at the surface. If hydrogen were to leak from an engineered reservoir and reach the surface, we might therefore expect the leak to manifest in a similar way. Physical features of hydrogen seepage thus have the potential to be a useful tool in monitoring engineered geological hydrogen storage sites. The three types of seepage we have identified have some unique physical characteristics (Fig. 9).

Springs can have some physical features caused by processes not directly related to hydrogen seepage (carbonate precipitation), whilst seepage from bedrock fractures have minimal physical characteristics – there are examples of gases spontaneously igniting at surface (Vacquand *et al.* 2018). Of the three types, seepage through sediments and soils is the only type of seepage that we identify to have broadly consistent visible physical features: subcircular depressions.

The physical origin of the observed subcircular features has yet to be resolved. Some studies from the subcircular depressions in Russia, USA, Mali and Brazil conclude that hydrogen-bearing gas seepage from depth results in localized rock alteration and subsidence or collapse (Zgonnik *et al.* 2015; Donzé *et al.* 2020), similar to offshore pockmark formation (Gay *et al.* 2019). Other authors have suggested that the depressions are not a result of hydrogen seepage, but caused by other environmental factors, and their presence provides a preferential flow for seeping hydrogen. For example, Moore *et al.* (2016) argue that the depressions located in the Carolina bays (#8–12) have migrated hundreds of metres over time (hundreds to thousands of

Natural hydrogen seeps as analogues

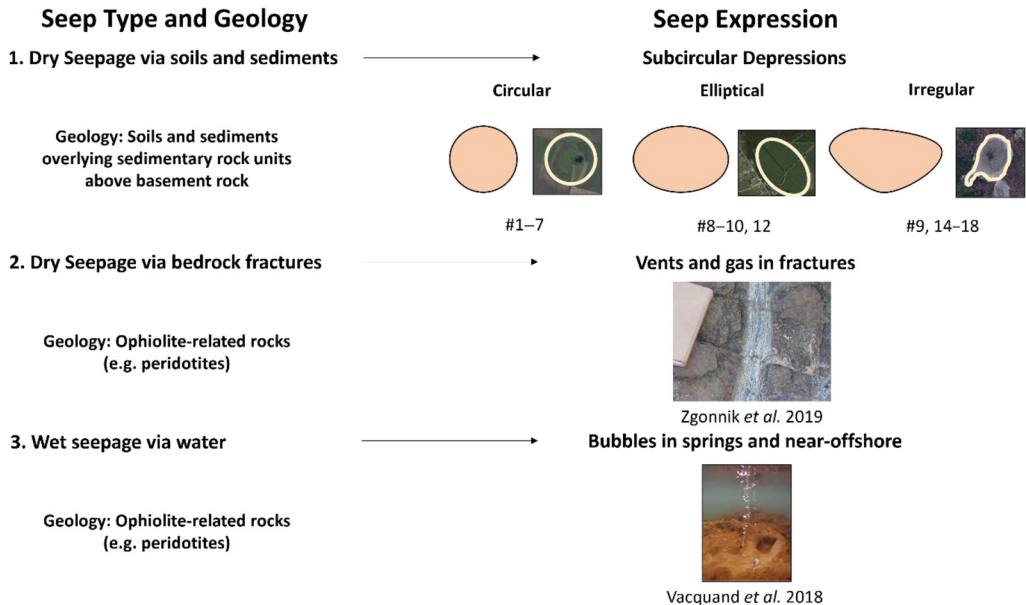


Fig. 9. Seep type, geological environment and surface expression of hydrogen seepage with example images and cartoons of typologies. (1) Subcircular depressions with three shapes – circular, elliptical and irregular. (2) Fractured rocks with diffusive flows of hydrogen (Zgonnik *et al.* 2019). (3) Bubbling seepage offshore, New Caledonia (#34). Source: images in (2) from Zgonnik *et al.* 2019 and (3) from Vacquand *et al.* (2018). Satellite photos in (1) from Google Maps.

years), likely in correlation to the prevailing wind direction, suggesting that these features are mobile, and otherwise unrelated to the presence of hydrogen. Similarly, the subcircular depressions in Brazil (#14, #15) are documented on geological maps as karstic lakes often with economic clay and spongillite sedimentary fill. Detailed studies of the sedimentation within some of these lakes (Almeida *et al.* 2010) have not yet identified any features associate with gas seepage, such as carbonate lenses or chimney structures, suggesting that they are not the result of gas seepage.

Previous work has suggested that large fault systems control hydrogen seep locations in Brazil (#14, 15, Coelho *et al.* 2008) and Australia (#16–18, Frery *et al.* 2021), either providing a conduit for deep-seated hydrogen to reach the surface, or to accumulate in subsurface reservoirs (Romeiro-Silva and Zalán 2005; Donzé *et al.* 2020). If the depressions are largely formed by karstic processes, fault systems present may control the location of some karstic lakes by enhancing subsurface fluid flow, and also provide a migration pathway. In Oman, there are fault systems which have been proposed as a migration pathway for hydrogen (Neal and Stanger 1983).

Previous authors have speculated that the location, alignment and axes of the subcircular shape of depressions are a result of structural features,

such as basement faults or local stress regimes (Larin *et al.* 2015; Zgonnik *et al.* 2015; Cathles and Prinzhofer 2020; Donzé *et al.* 2020; Frery *et al.* 2021). This has been observed previously at CO₂ vents (Bonini 2012). To explore this, we used World Stress Map (WSM) data (Heidbach *et al.* 2016) to compare the local stress regime with alignment of the orientation of subcircular hydrogen seeps (Table 5).

We find little compelling evidence that depression shape is controlled by stress orientation, but note that stress data are sparse. While there is some indication that the shape and orientation of depressions in USA, Russia and Brazil (#1–14) might be influenced by lacustrine and aeolian processes (Almeida *et al.* 2010; Zgonnik *et al.* 2015; Moore *et al.* 2016) particularly over long timescales, this does not explain the initial formation mechanism.

Hydrogen source, transformation and associated gases. Any robust monitoring programme needs to understand how leaked fluids may be modified as they migrate, react and accumulate in the subsurface at geological storage sites, and how they seep (Fig. 10).

Although hydrogen generation and consumption mechanisms in the subsurface are generally well understood (Sherwood Lollar *et al.* 2014; Panfilov

Table 5. Seep shape, axis orientation, stress orientation (S_{Hmax}) with distance from seep and prevailing wind direction

Location	Depression shape (axis orientation)	Stress (S_{Hmax}) orientation (distance from depression)	Prevailing wind direction
USA (Carolina Bays) (#8–12)	Elongate (30° to 45°, NNE–NE)	10° to c. 65° (160–515 km)	30–60° (NNE–ENE)
Russia (#1–7)	Circular	No data within 700 km of depressions	WSW–SSW
Australia (#16–18)	Some elongation (N–NW)	110° (c. 50 km)	East
Brazil (#13–14)	Some elongation (c. 120°, SE)	52–92° (155–250 km)	WNW–WSW

2016; Gregory *et al.* 2019), there is no clear agreement on the source(s) of hydrogen at the documented seeps (Larin *et al.* 2015; Zgonnik *et al.* 2015, 2019; Prinzhofer *et al.* 2018, 2019; Vacquand *et al.* 2018) (Table 6). Zgonnik *et al.* (2015) note that there must be a large-scale process that can generate and sustain significant quantities of hydrogen over time.

As bubbling gas seeps are found in ophiolitic settings, many authors have proposed serpentinization processes to be a key contributor to the production of hydrogen at these locations (Vacquand *et al.* 2018; Zgonnik *et al.* 2019; Zgonnik 2020). Based on major gas concentrations, stable isotopes and noble gas geochemistry, Vacquand *et al.* (2018) conclude that while low temperature, shallow

serpentinization is a dominant source of hydrogen in ophiolite systems, hydrogen associated with higher proportions of N_2 and CH_4 likely derives from a deeper, hotter source; this source is likely related to geothermal activity and mantle gases and indicates that deep hydrogen sources are a component of many ophiolite-hosted seeps. Figure 6 illustrates that the highest measured hydrogen concentration in a seep occurred in rock units that are not directly overlying ophiolitic rocks (where serpentinization takes place). This seep in Oman occurs in shales directly overlying Precambrian crust, which is a major source of hydrogen generated by water–rock interaction and radiolysis (Sherwood Lollar *et al.* 2014). This supports the hypothesis that

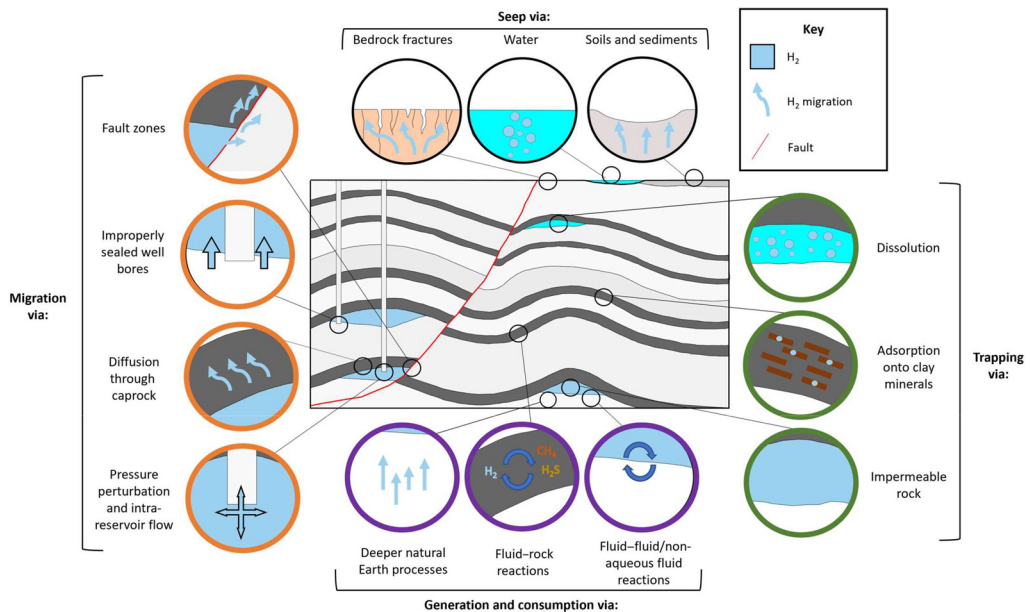


Fig. 10. Potential mechanisms for hydrogen generation and consumption (purple circles), trapping (green circles) and migration (orange circles) in the subsurface and seep expression at the surface (black circles). Source: adapted from Heinemann *et al.* (2021).

Natural hydrogen seeps as analogues

Table 6. *Interpreted sources of hydrogen from the literature*

Location	Interpreted source	Reference
Russia (#1–7)	Unknown (discussed multiple options)	Larin <i>et al.</i> (2015)
USA (Carolina) (#8–12)	Deep geochemical processes	Zgonnik <i>et al.</i> (2015)
Oman (#19– 29, #36–55)	Deep subsurface source (water interactions with Fe-rich minerals or serpentinization of mantle rock)	Zgonnik <i>et al.</i> (2019)
Turkey (#31, #58)	Serpentinization (CH ₄ is produced from the H ₂ reacting in presence of CO ₂ , Fischer–Tropsch type reactions)	Hosgörmez <i>et al.</i> (2008)
New Caledonia (#34, #35)	Serpentinization and deeper earth processes	Deville and Prinzhofer (2016); Vacquand <i>et al.</i> (2018)

Other locations (e.g. Philippines, Mali, Australia) presented in the results section discuss similar hydrogen sources and generation processes, but also with significant unknowns and uncertainty.

shallow serpentinization is not the sole source of hydrogen in many ophiolite-hosted seeps. Therefore, multiple sources of hydrogen can exist at the same seep location, where gases mix and, consequently, this increases complexity in source attribution.

As hydrogen migrates from source to surface, hydrogen can react both abiotically and biotically. Of the seeps presented in this paper, 45 have hydrogen occurring with methane, with examples #31 and #32 (Table 2), where methane is the dominant seeping gas. Methane can be formed by both abiotic and biotic processes that consume or transform hydrogen (Panfilov 2016; Gregory *et al.* 2019). Abiotic reactions include transformation to methane and other hydrocarbons at higher temperatures (>600°C) and at lower temperatures (e.g. Fischer–Tropsch-type synthesis, as low as 50°C, Sherwood Lollar *et al.* 2002, 2006, 2008). Recent studies at a geothermal field in Italy conclude that hydrogen produced at deeper levels of the crust is abiotically consumed at high temperatures to form CH₄ (Leila *et al.* 2021). Hydrogen can be biotically transformed to methane via methanogenesis. Hydrogenotrophic methanogen bacteria oxidize hydrogen in the presence of CO₂ to form CH₄ and H₂O in Sabatier’s reaction (Panfilov 2016). Hydrogen can also be consumed in other biotic reactions. Examples include: H₂S (sulfate reduction), acetate (acetogenesis), Fe²⁺ (iron-reduction) and H₂O (aerobic hydrogen oxidation) (Panfilov 2016; Gregory *et al.* 2019; Thaysen *et al.* 2021; Muhammed *et al.* 2022). Closer to surface, microbial communities in soils can act as hydrogen consumers (Conrad and Seiler 1981; Myagkiy *et al.* 2020a) and also produce hydrogen (Sugimoto *et al.* 1998).

For the studied seeps, the understanding of the hydrogen generation and reaction processes in ophiolite settings is broadly well understood and detailed (Vacquand *et al.* 2018). These seeps have mixed gases that can be traced to different sources

of hydrogen production in the subsurface and show transformation of hydrogen as it migrates from depth to surface. Figure 5 highlights the variability of gas mixtures that are reported for the seepage sites presented. These surface compositions do not necessarily reflect the original deep gas composition in the subsurface. The data that exist to make these assumptions for the seeps based in ophiolitic geology do not currently exist for seepage through soils and sediments that form subcircular depressions. These data are required to understand the source and migration of hydrogen from depth to surface – although these are difficult to collect due to the dilute and diffuse nature of the seeps.

The gas composition generated in the subsurface may differ to what reaches the surface – with implications for monitoring at engineered geological hydrogen storage sites. Controlled release experiments could be one option to study how well gas signatures are preserved as they migrate in the subsurface. Additionally, engineered hydrogen storage sites will likely have a purer quality of hydrogen than naturally produced, meaning pure hydrogen migration (no co-gases) could differ compared to hydrogen alongside other gases (CO₂, CH₄, N₂). However, mixtures at engineered storage sites could vary depending on the type of cushion gas used and this should be considered in any monitoring strategy.

Comparing hydrogen seepage to other gas seepage. The differences in hydrogen behaviour compared to other gases have implications for the monitoring of engineered geological hydrogen storage sites.

Hydrogen seeps share some characteristics with CO₂ and CH₄ seeps. CO₂ seeps are known to form in circular depressions (Roberts *et al.* 2015) and CH₄ seepage offshore leaves pockmarks (circular depressions) in seafloor sediments (e.g. Räss *et al.* 2018). CH₄ and CO₂ seeps migrate along faults and fractures, like hydrogen seeps (Zgonnik *et al.*

2019). Both hydrogen and CO₂ seeps (e.g. Roberts *et al.* 2019) have been found to occur as bubbles in spring waters. This distribution of these features at surface can then influence the spatial distribution of seepage (e.g. fracture-controlled distribution in Oman, Zgonnik *et al.* 2019).

Hydrogen has a low solubility in water: at 20°C the solubility of hydrogen is 0.0016 g kg⁻¹ water. At the same temperature CO₂ is around 1.4 g kg⁻¹ water. Hydrogen is less soluble than CO₂ in both mole fraction and mass fraction terms (Ennis-King 2021). This explains why hydrogen is likely found bubbling in water at the surface, as hydrogen is less soluble than other gases, so in the presence of water, hydrogen concentration may be elevated compared to other gases. However, hydrogen can be found dissolved in shallow low-salinity aquifers. Frery *et al.* (2021) note that the high geothermal gradient in their study region in Australia (40°C km⁻¹), coupled with the low salinity of the groundwater systems, means increased hydrogen solubility would result in high concentrations of aqueous phase hydrogen at shallower depths (<1 km). Thus, hydrogen can migrate in both gaseous (via major faults) and aqueous phase (shallow-depth low salinity aquifers). Seasonal changes in water table or groundwater conditions could alter these hydrogen migration pathways, as at sites of CO₂ seepage (Roberts *et al.* 2015), and clearly structures (e.g. faults, fractures) effect fluid flow in both hydrogen and CO₂ seeps (e.g. Roberts *et al.* 2017, 2019).

Hydrogen seepage sites do share some characteristics with other gas seeps; however, there are notable differences. Hydrogen may pose a different risk compared to CO₂ or CH₄ seepage. Unlike CO₂, which is denser than air, hydrogen will not accumulate at high concentrations in topographic depressions, posing less of a safety risk. However, hydrogen seepage sites are often associated with vegetation loss and decay of organic matter (Sukhanova *et al.* 2013), meaning there may be other hazards from hydrogen seepage. Some hydrogen seepage sites are associated with spontaneously igniting gases that can burn for thousands of years. These sites are dominated by methane which is the primary source for the ignition. Mostly notably, sites of hydrogen seepage differ from sites of CO₂ seepage in that hydrogen can be transformed before reaching the surface due to subsurface reactions (see section 'Hydrogen source, transformation and associated gases').

Recommendations for engineered geological hydrogen storage

Our findings on natural hydrogen analogues have implications for monitoring of engineered hydrogen stores.

For engineered stores, the pressure conditions of a storage site will likely change during injection and withdrawal cycles (Heinemann *et al.* 2021), therefore a cyclic emission style might be expected. In addition, hydrogen seepage from engineered stores will vary both predictably (atmospheric and diurnal changes) and perhaps less predictably, such as when biological communities establish – with implications for effective monitoring of engineered geological hydrogen storage sites. If a leak from engineered storage was to be established and reach the surface, manifesting as a diffuse seep, the observations from many of the studied natural seeps suggest that short-term (diurnal, seasonal) and long-term variation in hydrogen seepage is to be expected (Prinzhofer *et al.* 2019; Myagkiy *et al.* 2020a, b; Frery *et al.* 2021; Moretti *et al.* 2021a, b). This means that background monitoring over an extended time (several weeks to capture diurnal cycles, but up to two years to capture seasonal variation) should be established prior to hydrogen storage. Other useful data could include weather data (e.g. temperature, humidity, air pressure) and consider aspects such as tides.

The surface expression of hydrogen seepage varies depending on the geology and sediment cover. The type of hydrogen seepage and the surface expression (if any), and, therefore, appropriate monitoring approaches, will be controlled to an extent by the exposed bedrock and superficial deposits. Our findings suggest that; where seepage occurs through soils and unconsolidated sediments, a physical expression will establish, assisting the identification of leakage, and, thus, monitoring approaches such as remote sensing image analysis could be appropriate. Monitoring in subcircular depressions should note that hydrogen concentrations are spatially variable (Figs 3 & 4), and hydrogen flux may occur outside the boundaries of the subcircular depression. Within ophiolitic or subduction complexes, where there is no soil or sediment cover, seepage is via fractured rocks and springs. Different monitoring approaches will be required, but, as with natural CO₂ seeps (Roberts *et al.* 2019), monitoring approaches might target springs and water courses, or topographic lows. Springs could be used to locate monitoring equipment and monitor gases. Seepage may be detected by periodic groundwater (aquifer) sampling and analysis (e.g. Etiope *et al.* 2017), by measuring molecular composition of dissolved gases, as well as water properties (e.g. pH and Eh).

Owing to the mobility, reactivity and consumption of hydrogen in the subsurface, both abiotically and biotically, challenges for monitoring hydrogen are different compared to other more developed geological gas storage technologies (e.g. CO₂, CH₄ storage). Thus far, we have considered monitoring of gas leaving the reservoir due to buoyancy

forces. However, hydrogen could also be lost from the reservoir via transformation into different gases (e.g. CH₄) by reducing fluid or rock reactions and microbial action. Hydrogen can also be trapped on mineral surfaces (e.g. clay minerals) (Truche *et al.* 2018) and consumed by soil bacteria if a leak were to reach the surface (Conrad and Seiler 1981; Myagkiy *et al.* 2020a). These reactions could result in hydrogen leakage from a reservoir being difficult to detect at the surface. Consequently, subsurface (direct) monitoring techniques (e.g. monitoring of the reservoir integrity and subsurface borehole monitoring techniques) will likely be crucial to detect any hydrogen leakage early and with a higher degree of certainty. Highly sensitive monitoring approaches may be required to detect hydrogen seepage; although hydrogen has a low atmospheric concentration, the highly mobile and buoyant nature of hydrogen means that hydrogen dispersal will be high. Hydrogen plume dispersal studies will be important to understand how hydrogen may behave if released at surface and how to appropriately measure and monitor for this. Monitoring for common transformation gases (e.g. CH₄) and analysing the isotopic composition could be appropriate in environments where hydrogen is able to be transformed into other compounds.

Key research and data gaps

Natural analogues of CO₂ seepage and storage have been used for decades to provide information on seep rate, flux, subsurface geometries, CO₂ migration and trapping and more (Irwin and Barnes 1980; Pearce *et al.* 1996, 2004; Holloway *et al.* 2007; Miodic *et al.* 2013; Roberts *et al.* 2017, 2019). This information has been used to make robust recommendations for effective MMV strategies. For sites of hydrogen seepage and accumulation, we are limited in the data available and by the data reported. There are: (a) a general lack of reported data for natural hydrogen seepage and accumulation. This is related to (b) broader issues around the field data collection methodologies (e.g. drilling, measurements from only one point in time) and (c) uncertainty is introduced by simplifying and estimating values (e.g. area, porosity) for calculating hydrogen fluxes from seep rates and concentrations. Finally, (d) studies must consider and rule out biological sources of hydrogen.

There are a combination of reasons regarding a lack of reported data on hydrogen seepage and accumulations. Firstly, hydrogen has different physico-chemical properties when compared to other gases, meaning the overall risk and hazard differs and is perhaps reduced – which may explain a general lack of reported sites of seepage. Secondly, the lack of any global exploration programme for natural hydrogen means that there may be seepage sites or

accumulations that exist that have not yet been discovered. This could be because they may occur in different locations to conventional hydrocarbon resources, both geographically and in terms of depth in the subsurface. Many of the examples of hydrogen seeps presented in this paper suggest a deep-seated source of hydrogen, and the Precambrian crust has been established as a significant reservoir of hydrogen (Sherwood Lollar *et al.* 2014). Only in the late 2010s and early 2020s have both academia and industry started to pursue natural hydrogen as a possible low-carbon energy resource; however, there is a rapid increase in interest in this area. New companies, for example, Natural Hydrogen Energy LLC (NH2E 2022), have been created that are dedicated to prospecting and drilling for natural hydrogen accumulations in the subsurface, while existing well-established companies are expanding from other operations to consider subsurface hydrogen storage and natural hydrogen. Further, governments are now permitting for natural hydrogen exploration (e.g. Government of South Australia 2022). Thirdly, we have discussed the multiple ways in which hydrogen can react in the subsurface before reaching the surface – potentially leading to its transformation or consumption. Finally, the highly mobile nature of hydrogen and the restricted range of conditions that are likely to cause its accumulation in subsurface reservoirs might simply mean that there are very few hydrogen-bearing gas seeps.

Hydrogen concentration has been observed to vary throughout the day (Prinzhofer *et al.* 2019; Moretti *et al.* 2021a), and these temporal variations introduce significant uncertainty in estimating seep and flux rates. Further, detailed information is missing at many sites around the rate of emission.

Many of the reported seeps measured hydrogen in soil gas wells produced by drilling. Hydrogen may be produced during drilling due to cracking of organic matter (Halas *et al.* 2021) and/or water (Kita *et al.* 1982). A circular depression in South Gironde, France was initially thought to be a hydrogen seep, based on early drilling studies, but was ruled out after it was found that hydrogen could be artificially generated in the soil during drilling (Halas *et al.* 2021). Halas *et al.* (2021) highlight the importance of developing a robust sampling method and note that studies of natural hydrogen seepage should avoid drilling in the sampling process. Of the studies discussed in this paper, only Zgonnik *et al.* (2015, 2019) specifically address this issue and state that significant flushing time was allowed between measurements to ensure that any hydrogen was not associated with drilling. Zgonnik *et al.* (2019) argue that drilling is not responsible for the hydrogen measured in their study due to the lack of hydrogen in drilled borehole samples from unfractured rocks in the area, but this conclusion

does not account for potential variation in water and organic matter content that may act as a source of drilling-induced hydrogen. Other papers are unclear regarding the potential for results to be affected by drilling-induced hydrogen. Consequently, we recommend a standardized and effective methodology for the collection of field data, that accounts for the need to measure differently depending on the style of seepage and rules out hydrogen production via sampling methodology. Recent, more detailed studies have made progress in this respect, for example, studies in Brazil have conducted detailed analysis of hydrogen seepage. These explore the meaning of pulsed emissions (Cathles and Prinzhofer 2020) and longer-term monitoring of a depression (Moretti *et al.* 2021a). These monitoring programmes use multiple sensors, deployed over a time interval to get an idea of the spatial and temporal variation in seepage. This methodology is more effective than measurements from one point in time that are spatially constrained. Thus, we recommend that sufficient sensors are deployed to elucidate the spatial variation in seepage (the actual number will depend on the seep characteristics and size, but as a rule of thumb we recommend a spacing of no more than tens of metres between sensors, e.g. Moretti *et al.* 2021a) and that these are deployed over a period (i.e. months at a minimum, but ideally one or two years) to appropriately capture diurnal and seasonal temporal variation in seepage. Additionally, results from Larin *et al.* (2015) and Zgonnik *et al.* (2015) analyse soil gas using pumped measurement protocols, but instead flux chamber methods should be deployed to quantify hydrogen flux rates more accurately. Lastly, drilling should be avoided to ensure that no hydrogen is produced by this method as evidenced by Kita *et al.* (1982) and Halas *et al.* (2021), which would subsequently influence measured hydrogen concentrations.

There is an additional problem of consistency in the data reported in the published literature. This can make comparisons between different datasets, and identifying contributions of biologically produced hydrogen, problematic. Often data are averaged (e.g. concentrations) and assumptions are made (e.g. area, porosity), which introduces uncertainty into the final flux estimates (e.g. Cathles and Prinzhofer 2020; Donzé *et al.* 2020). Therefore, we recommend consistency in the reporting of data, as well as analysis of the spatial and temporal evolution of hydrogen seepage. For each seepage site, the spatial area of seepage should be quantified (e.g. for sub-circular depressions the radius/diameter of the depression) as well as the cross-sectional profile of the seepage area or profiles for non-circular seeps. Data such as the surface geology and type and quantity of gases present should be recorded. Where possible, gas fluxes should be recorded and any

information about the source of hydrogen and the temporal evolution of seepage (e.g. time of onset of seepage) should be recorded. Additionally, the methodology used should be described in enough detail to allow understanding of the conditions in which samples (e.g. gas concentrations) were collected. This includes whether samples were taken at the surface (in air), in the subsurface (in soils or rock) or in/near water. Subsurface samples should note the depth at which they were taken and the means to reach this depth (i.e. drilling or otherwise). Samples near or from water (e.g. springs) should collect basic data on the water properties (at a minimum, temperature, pH and Eh should be recorded). Other data such as the time samples were collected, the season in which samples were collected and the weather at the time of sampling should be noted. Other environmental factors which might influence the collected data should be noted (e.g. vegetation, land use). Further work is needed to understand the formation of surface sub-circular depressions, controls on their size and shape as well as how any orientation relates to subsurface structural features.

Studies of CO₂ seeps in Daylesford (Australia) have highlighted the importance of different spatial scales of analysis, as well as the importance of surface processes in controlling seepage locations and rates (Roberts *et al.* 2019). This highlights the importance of understanding surface processes that can influence how fluids seep and how they may influence surface seep expression, ensuring that the focus is not fully on the migration from the deep subsurface. This is an area to consider in further studies.

Although there is a good understanding of natural methods of hydrogen production in the subsurface, the discussions highlight that there are still many unknowns regarding the source of the hydrogen in many of the examples presented. From source to surface, the migration of hydrogen can be baffled by several processes that can transform or trap hydrogen. Understanding migration pathways to surface, as well as potential baffles, is important in assessing the risk of hydrogen both exiting the storage reservoir and reaching the surface. There is only one published example of a natural hydrogen accumulation in Mali. While there is a documented seep in Mali (#13, Table 1 Prinzhofer *et al.* 2018), it is located 218 km away from the production well. The lack of documented seeps directly above or close to this accumulation suggests that the accumulation must have an appropriate seal that is stopping hydrogen migrating to the Earth's surface. The lack of examples of natural hydrogen storage means this one analogue in the literature of natural hydrogen storage (Prinzhofer *et al.* 2018) is likely not analogous for all future engineered hydrogen storage sites, or

indeed any other natural hydrogen accumulations. This is similar to the findings of Roberts *et al.* (2017) who note that natural CO₂ reservoirs are not direct analogues of CO₂ storage sites due to the differences in processes and operation, but do provide valuable learnings for MMV. Prospecting for new natural hydrogen seepage and accumulations could help to develop understanding of seepage pathways and barriers. This will be important for the effective site selection and monitoring of engineered geological hydrogen storage. However, in all cases, the source of natural hydrogen and the migration pathways are poorly understood, and so robust implications for site selection of hydrogen stores cannot be made.

Conclusions

To date, natural hydrogen seepage sites have been largely unreported and understudied. Furthermore, sites of hydrogen seepage at the surface have only been studied by those primarily interested in prospecting for natural hydrogen accumulations in the subsurface. However, natural hydrogen seepage and accumulation can inform appropriate monitoring approaches for engineered geological hydrogen storage.

We know from hydrogen seepage that seep characteristics are determined by local geological and hydrological conditions, specifically whether hydrogen gas is seeping through soils and unconsolidated sediments, fractured bedrock or water (e.g. springs). Where hydrogen seeps through soils and sediments, seeps manifest as sub-circular depressions with patchy flux, and the spatial extent of the seep controls the seep rate. Where hydrogen seeps through bedrock fractures or into springs, gas emissions are highly localized, with small spatial footprint of seepage. In the studied seeps, hydrogen seepage is known to seep to the surface over extended periods of time (years, as a minimum).

Monitoring approaches for engineered hydrogen stores should therefore be tailored according to the exposed geology and hydrological conditions. We find similarities in the controls on seep location and characteristics between hydrogen seeps and CO₂ seeps, which have been more widely studied to inform geological CO₂ storage. However, compared to CO₂, hydrogen is more readily dispersed because of its high mobility (due to small size and low density), and so maximum concentrations of hydrogen in gas streams that reach the surface are typically lower than CO₂ concentrations at CO₂ seeps.

In all cases, hydrogen is typically co-emitted with other naturally occurring gases such as CO₂, CH₄ and small amounts of trace hydrocarbons or noble gases, with CH₄ being the most dominant co-emitted

gas in most cases presented here. Hydrogen can be consumed or transformed in the subsurface, and so the quantity of leaked hydrogen might be greatly attenuated before it reaches the Earth's surface. As such, subsurface monitoring approaches to detect hydrogen, or tools that also monitor for co-gases, could be appropriate in environments that promote the transformation of hydrogen to other compounds.

In all cases, the source of hydrogen and the migration pathways are uncertain, and so robust implications for site selection of hydrogen stores cannot be made. We recommend: (1) a standardized and effective methodology for the collection of field data, that accounts for the need to measure differently depending on the style of seepage; (2) consistency in the reporting of data, analysis of the spatial and temporal evolution of hydrogen seepage and consideration of how surface processes may influence surface seep expression; (3) further work to understand the initial formation of surface sub-circular depressions, controls on their size and shape as well as how any orientation relates to subsurface structural features; and (4) further work to detail and mitigate hydrogen seepage risks.

Acknowledgements We would like to thank reviewers (Linda Stalker and one anonymous reviewer) for thorough and constructive reviews.

Competing interests The authors declare that they have no known competing financial interests or personal relationships that could have appeared to influence the work reported in this paper.

Author contributions **CJM**: conceptualization (lead), data curation (lead), formal analysis (lead), investigation (lead), methodology (lead), project administration (lead), visualization (lead), writing – original draft (lead), writing – review & editing (lead); **JJR**: conceptualization (supporting), formal analysis (supporting), methodology (supporting), supervision (lead), visualization (supporting), writing – original draft (supporting), writing – review & editing (supporting); **GJ**: conceptualization (supporting), formal analysis (supporting), investigation (supporting), methodology (supporting), project administration (supporting), supervision (supporting), visualization (supporting), writing – original draft (supporting), writing – review & editing (supporting); **KE**: conceptualization (supporting), formal analysis (supporting), supervision (supporting), visualization (supporting), writing – review & editing (supporting); **SF**: conceptualization (supporting), formal analysis (supporting), methodology (supporting), visualization (supporting), writing – review & editing (supporting); **ZKS**: conceptualization (supporting), formal analysis (supporting), methodology (supporting), supervision (supporting), visualization (supporting), writing – review & editing (supporting).

Funding CM is funded by the Engineering and Physical Sciences Research Council (EPSRC) funded studentship (grant number EP/R513349/1). KE is funded by the Engineering and Physical Sciences Research Council (EPSRC) funded research project ‘HyStorPor’ (grant number EP/S027815/1) and from the Fuel Cells and Hydrogen 2 Joint Undertaking (now Clean Hydrogen Partnership) HyUsPre project under grant agreement No. 101006632.

Data availability All data underpinning this publication are openly available from the University of Strathclyde KnowledgeBase at: <https://doi.org/10.15129/89bae037-9174-4556-883b-86e6c3216590>

References

- Abrajano, T.A., Sturchio, N.C., Bohlke, J.K., Lyon, G.L., Poreda, R.J. and Stevens, C.M. 1988. Methane-hydrogen gas seeps, Zambales Ophiolite, Philippines: deep or shallow origin?. *Chemical Geology*, **71**, 211–222, [https://doi.org/10.1016/0009-2541\(88\)90116-7](https://doi.org/10.1016/0009-2541(88)90116-7)
- Almeida, A.C.S., Varajão, A.F.D.C., Gomes, N.S., Varajão, C.A.C. and Volkmer-Ribeiro, C. 2010. Characterization and origin of spongillite-hosting sediment from João Pinheiro, Minas Gerais, Brazil. *Journal of South American Earth Sciences*, **29**, 439–453, <https://doi.org/10.1016/j.jsames.2009.09.006>
- Bonini, M. 2012. Mud volcanoes: indicators of stress orientation and tectonic controls. *Earth Science Reviews*, **115**, 121–152, <https://doi.org/10.1016/j.earscirev.2012.09.002>
- Buzek, F., Onderka, V., Vančura, P. and Wolf, I. 1994. Carbon isotope study of methane production in a town gas storage reservoir. *Fuel*, **73**, 747–752, [https://doi.org/10.1016/0016-2361\(94\)90019-1](https://doi.org/10.1016/0016-2361(94)90019-1)
- Carden, P.O. and Paterson, L. 1979. Physical, chemical and energy aspects of underground hydrogen storage. *International Journal of Hydrogen Energy*, **4**, 559–569, [https://doi.org/10.1016/0360-3199\(79\)90083-1](https://doi.org/10.1016/0360-3199(79)90083-1)
- Cathles, L. and Prinzhofer, A. 2020. What pulsating H₂ emissions suggest about the H₂ resource in the Sao Francisco Basin of Brazil. *Geosciences*, **10**, 149, <https://doi.org/10.3390/geosciences10040149>
- Coelho, J.C.C., Martins-Neto, M.A. and Marinho, M.S. 2008. Estilos estruturais e evolução tectônica da porção mineira da bacia proterozóica do São Francisco. *Revista Brasileira de Geociências*, **38**, 149–165, <https://doi.org/10.25249/0375-7536.2008382S149165>
- Conrad, R. and Seiler, W. 1980. Contribution of hydrogen production by biological nitrogen fixation to the global hydrogen budget. *Journal of Geophysical Research*, **85**, 5493, <https://doi.org/10.1029/JC085iC10p05493>
- Conrad, R. and Seiler, W. 1981. Decomposition of atmospheric hydrogen by soil microorganisms and soil enzymes. *Soil Biology and Biochemistry*, **13**, 43–49, [https://doi.org/10.1016/0038-0717\(81\)90101-2](https://doi.org/10.1016/0038-0717(81)90101-2)
- Coveney, R.M., Goebel, E.D., Zeller, E.J., Dreschhoff, G.A.M. and Angino, E.E. 1987. Serpentinization and the origin of hydrogen gas in Kansas. *AAPG Bulletin*, **71**, 39–48 <https://doi.org/10.1306/94886D3F-1704-11D7-8645000102C1865D>
- Deville, E. and Prinzhofer, A. 2016. The origin of N₂–H₂–CH₄-rich natural gas seepages in ophiolitic context: a major and noble gases study of fluid seepages in New Caledonia. *Chemical Geology*, **440**, 139–147, <https://doi.org/10.1016/j.chemgeo.2016.06.011>
- Donzé, F.V., Truche, L., Shekari Namin, P., Lefeuvre, N. and Bazarkina, E.F. 2020. Migration of natural hydrogen from deep-seated sources in the São Francisco Basin, Brazil. *Geosciences*, **10**, 346, <https://doi.org/10.3390/geosciences10090346>
- Ennis-King, J. 2021. *Underground storage of hydrogen: mapping out the options for Australia (RP1.1-04)*. Future Fuels Cooperative Research Centre report, <https://www.futurefuelsrc.com/project/underground-storage-of-hydrogen-mapping-out-the-options-for-australia-rp1-1-04/>
- Etiopie, G. and Sherwood Lollar, B. 2013. Abiotic methane on Earth. *Reviews of Geophysics*, **51**, 276–299, <https://doi.org/10.1002/rog.20011>
- Etiopie, G., Samardžić, N., Grassa, F., Hrvatović, H., Miošić, N. and Skopljak, F. 2017. Methane and hydrogen in hyperalkaline groundwaters of the serpentinized Dinaride ophiolite belt, Bosnia and Herzegovina. *Applied Geochemistry*, **84**, 286–296, <https://doi.org/10.1016/j.apgeochem.2017.07.006>
- Frery, E., Langhi, L., Maison, M. and Moretti, I. 2021. Natural hydrogen seeps identified in the North Perth Basin, Western Australia. *International Journal of Hydrogen Energy*, **46**, 31158–31173, <https://doi.org/10.1016/j.ijhydene.2021.07.023>
- Gay, A., Lopez, M., Potdevin, J.-L., Vidal, V., Varas, G., Favier, A. and Tribouillard, N. 2019. 3D morphology and timing of the giant fossil pockmark of Beauvoisin, SE Basin of France. *Journal of the Geological Society, London*, **176**, 61–77, <https://doi.org/10.1144/jgs2018-064>
- Getzin, S., Yizhaq, H. and Tschinkel, W.R. 2021. Definition of ‘fairy circles’ and how they differ from other common vegetation gaps and plant rings. *Journal of Vegetation Science*, **32**, e13092, <https://doi.org/10.1111/jvs.13092>
- Government of South Australia 2022. Gold Hydrogen natural hydrogen exploration, <https://www.energymining.sa.gov.au/industry/energy-resources/regulation/projects-of-public-interest/gold-hydrogen-natural-hydrogen-exploration#summary> [last accessed 16 June 2022]
- Gregory, S.P., Barnett, M.J., Field, L.P. and Milodowski, A.E. 2019. Subsurface microbial hydrogen cycling: natural occurrence and implications for industry. *Microorganisms*, **7**, 1–27, <https://doi.org/10.3390/microorganisms7020053>
- Halas, P., Dupuy, A., Franceschi, M., Bordmann, V., Fleury, J.M. and Duclerc, D. 2021. Hydrogen gas in circular depressions in South Gironde, France: flux, stock, or artefact? *Applied Geochemistry*, **127**, 104928, <https://doi.org/10.1016/j.apgeochem.2021.104928>
- Hanley, E.S., Deane, J.P. and Gallachóir, B.Ó. 2018. The role of hydrogen in low carbon energy futures—a review of existing perspectives. *Renewable and Sustainable Energy Reviews*, **82**, 3027–3045, <https://doi.org/10.1016/j.rser.2017.10.034>
- Heidbach, O., Rajabi, M., Reiter, K. and Ziegler, M. 2016. World Stress Map Database Release 2016. V. 1.1. GFZ

Natural hydrogen seeps as analogues

- Data Services, <https://doi.org/10.5880/WSM.2016.001>
- Heinemann, N., Booth, M.G., Haszeldine, R.S., Wilkinson, M., Scafidi, J. and Edlmann, K. 2018. Hydrogen storage in porous geological formations—onshore play opportunities in the midland valley (Scotland, UK). *International Journal of Hydrogen Energy*, **43**, 20861–20874, <https://doi.org/10.1016/j.ijhydene.2018.09.149>
- Heinemann, N., Alcalde, J. *et al.* 2021. Enabling large-scale hydrogen storage in porous media – the scientific challenges. *Energy & Environmental Science*, **14**, 853–864, <https://doi.org/10.1039/D0EE03536J>
- Holloway, S., Pearce, J.M., Hards, V.L., Ohsumi, T. and Gale, J. 2007. Natural emissions of CO₂ from the geosphere and their bearing on the geological storage of carbon dioxide. *Energy*, **32**, 1194–1201, <https://doi.org/10.1016/j.energy.2006.09.001>
- Hosgörmez, H., Etiopie, G. and Yalçın, M.N. 2008. New evidence for a mixed inorganic and organic origin of the Olympic Chimaera fire (Turkey): a large onshore seepage of abiogenic gas. *Geofluids*, **8**, 263–273, <https://doi.org/10.1111/j.1468-8123.2008.00226.x>
- IEA 2013. *Energy Technology Roadmap Hydrogen and Fuel Cells*. JRC Scientific Policy Report.
- Irwin, W.P. and Barnes, I. 1980. Tectonic relations of carbon dioxide discharges and earthquakes. *Journal of Geophysical Research*, **85**, 3115–3121, <https://doi.org/10.1029/JB085iB06p03115>
- Kita, I., Matsuo, S. and Wakita, H. 1982. H₂ generation by reaction between H₂O and crushed rock: an experimental study on H₂ degassing from the active fault zone. *Journal of Geophysical Research: Solid Earth*, **87**, 10789–10795, <https://doi.org/10.1029/JB087iB13p10789>
- Larin, N., Zgonnik, V., Rodina, S., Deville, E., Prinzhofer, A. and Larin, V.N. 2015. Natural molecular hydrogen seepage associated with surficial, rounded depressions on the European craton in Russia. *Natural Resources Research*, **24**, 369–383, <https://doi.org/10.1007/s11053-014-9257-5>
- Lazarou, S., Vita, V., Diamantaki, M., Karanikolou-Karra, D., Fragoyiannis, G., Makridis, S. and Ekonomou, L. 2018. A simulated roadmap of hydrogen technology contribution to climate change mitigation based on Representative Concentration Pathways considerations. *Energy Science & Engineering*, **6**, 116–125, <https://doi.org/10.1002/ese3.194>
- Leila, M., Lévy, D. *et al.* 2021. Origin of continuous hydrogen flux in gas manifestations at the Larderello geothermal field, Central Italy. *Chemical Geology*, **585**, 120564, <https://doi.org/10.1016/j.chemgeo.2021.120564>
- Meredith, L.K., Commene, R., Munger, J.W., Dunn, A., Tang, J., Wofsy, S.C. and Prinn, R.G. 2014. Ecosystem fluxes of hydrogen: a comparison of flux-gradient methods. *Atmospheric Measurement Techniques*, **7**, 2787–2805, <https://doi.org/10.5194/amt-7-2787-2014>
- Miocić, J.M., Gilfillan, S.M., McDermott, C. and Haszeldine, R.S. 2013. Mechanisms for CO₂ leakage prevention – a global dataset of natural analogues. *Energy Procedia*, **40**, 320–328, <https://doi.org/10.1016/j.egypro.2013.08.037>
- Miocić, J.M., Gilfillan, S.M., Roberts, J.J., Edlmann, K., McDermott, C.I. and Haszeldine, R.S. 2016. Controls on CO₂ storage security in natural reservoirs and implications for CO₂ storage site selection. *International Journal of Greenhouse Gas Control*, **51**, 118–125, <https://doi.org/10.1016/j.ijggc.2016.05.019>
- Moore, C.R., Brooks, M.J., Mallinson, D.J., Parham, D.R., Ivester, A.H. and Feathers, J.K. 2016. The Quaternary evolution of Herndon Bay, a Carolina Bay on the coastal plain of North Carolina (USA): implications for paleoclimate and oriented lake genesis. *Southeastern Geology*, **51**.
- Moretti, I., Prinzhofer, A., Françolin, J., Pacheco, C., Rosanne, M., Rupin, F. and Mertens, J. 2021a. Long-term monitoring of natural hydrogen superficial emissions in a Brazilian cratonic environment. Sporadic large pulses v. daily periodic emissions. *International Journal of Hydrogen Energy*, **46**, 3615–3628, <https://doi.org/10.1016/j.ijhydene.2020.11.026>
- Moretti, I., Brouilly, E., Loiseau, K., Prinzhofer, A. and Deville, E. 2021b. Hydrogen emanations in intracratonic areas: new guide lines for early exploration basin screening. *Geosciences*, **11**, 145, <https://doi.org/10.3390/geosciences11030145>
- Morrill, P.L., Kuenen, J.G. *et al.* 2013. Geochemistry and geobiology of a present-day serpentinization site in California: the Cedars. *Geochimica et Cosmochimica Acta*, **109**, 222–240, <https://doi.org/10.1016/j.gca.2013.01.043>
- Mouli-Castillo, J., Heinemann, N. and Edlmann, K. 2021. Mapping geological hydrogen storage capacity and regional heating demands: an applied UK case study. *Applied Energy*, **283**, 116348, <https://doi.org/10.1016/j.apenergy.2020.116348>
- Muhammed, N.S., Haq, B., Al Shehri, D., Al-Ahmed, A., Rahman, M.M. and Zaman, E. 2022. A review on underground hydrogen storage: insight into geological sites, influencing factors and future outlook. *Energy Reports*, **8**, 461–499, <https://doi.org/10.1016/j.egy.2021.12.002>
- Myagkiy, A., Brunet, F. *et al.* 2020a. H₂ dynamics in the soil of a H₂-emitting zone (São Francisco Basin, Brazil): microbial uptake quantification and reactive transport modelling. *Applied Geochemistry*, **112**, 104474, <https://doi.org/10.1016/j.apgeochem.2019.104474>
- Myagkiy, A., Moretti, I. and Brunet, F. 2020b. Space and time distribution of subsurface H₂ concentration in so-called ‘fairy circles’: insight from a conceptual 2-D transport model. *BSGF-Earth Sciences Bulletin*, **191**, 13, <https://doi.org/10.1051/bsgf/2020010>
- Neal, C. and Stanger, G. 1983. Hydrogen generation from mantle source rocks in Oman. *Earth and Planetary Science Letters*, **66**, 315–320, [https://doi.org/10.1016/0012-821X\(83\)90144-9](https://doi.org/10.1016/0012-821X(83)90144-9)
- NH2E 2022. Natural Hydrogen Energy LLC, <http://nh2e.com/> [last accessed 16 June 2022]
- Novelli, P.C., Lang, P.M., Masarie, K.A., Hurst, D.F., Myers, R. and Elkins, J.W. 1999. Molecular hydrogen in the troposphere: global distribution and budget. *Journal of Geophysical Research*, **104**, 30427, <https://doi.org/10.1029/1999JD900788>
- Panfilov, M. 2016. Underground and pipeline hydrogen storage. *Woodhead Publishing Series in Energy*, **2**, 91–115, <https://doi.org/10.1016/B978-1-78242-362-1.00004-3>

- Pearce, J.M., Holloway, S., Wacker, H., Nelis, M.K., Rochelle, C. and Bateman, K. 1996. Natural occurrences as analogues for the geological disposal of carbon dioxide. *Energy Conversion and Management*, **37**, 1123–1128, [https://doi.org/10.1016/0196-8904\(95\)00309-6](https://doi.org/10.1016/0196-8904(95)00309-6)
- Pearce, J., Czernichowski-Lauriol, I. *et al.* 2004. A review of natural CO₂ accumulations in Europe as analogues for geological sequestration. *Geological Society, London, Special Publications*, **233**, 29–41, <https://doi.org/10.1144/GSL.SP.2004.233.01.04>
- Piovan, S.E. and Hodgson, M.E. 2017. How many Carolina bays? An analysis of Carolina bays from USGS topographic maps at different scales. *Cartography and Geographic Information Science*, **44**, 310–326, <https://doi.org/10.1080/15230406.2016.1162670>
- Prinzhofer, A., Cissé, C.S.T. and Diallo, A.B. 2018. Discovery of a large accumulation of natural hydrogen in Bourakebougou (Mali). *International Journal of Hydrogen Energy*, **43**, 19315–19326, <https://doi.org/10.1016/j.ijhydene.2018.08.193>
- Prinzhofer, A., Moretti, I., Francolin, J., Pacheco, C., d'Agostino, A., Werly, J. and Rupin, F. 2019. Natural hydrogen continuous emission from sedimentary basins: the example of a Brazilian H₂-emitting structure. *International Journal of Hydrogen Energy*, **44**, 5676–5685, <https://doi.org/10.1016/j.ijhydene.2019.01.119>
- Räss, L., Simon, N.S. and Podladchikov, Y.Y. 2018. Spontaneous formation of fluid escape pipes from subsurface reservoirs. *Scientific Reports*, **8**, 1–11, <https://doi.org/10.1038/s41598-018-29485-5>
- Roberts, J.J. and Stalker, L. 2020. What have we learnt about CO₂ leakage from CO₂ release field experiments, and what are the gaps for the future? *Earth-Science Reviews*, **209**, 102939, <https://doi.org/10.1016/j.earscirev.2019.102939>
- Roberts, J.J., Wood, R.A., Wilkinson, M. and Haszeldine, S. 2015. Surface controls on the characteristics of natural CO₂ seeps: implications for engineered CO₂ stores. *Geofluids*, **15**, 453–463, <https://doi.org/10.1111/gfl.12121>
- Roberts, J.J., Wilkinson, M., Naylor, M., Shipton, Z.K., Wood, R.A. and Haszeldine, R.S. 2017. Natural CO₂ sites in Italy show the importance of overburden geopressure, fractures and faults for CO₂ storage performance and risk management. *Geological Society, London, Special Publications*, **458**, 181–211, <https://doi.org/10.1144/SP458.14>
- Roberts, J.J., Stalker, L., Shipton, Z. and Burnside, N. 2018. What have we learnt about CO₂ leakage in the context of commercial-scale CCS?. *14th Greenhouse Gas Control Technologies Conference Melbourne*, 21–26.
- Roberts, J.J., Leplastrier, A., Feitz, A.J., Shipton, Z.K., Bell, A.F. and Karolytè, R. 2019. Structural controls on the location and distribution of CO₂ emission at a natural CO₂ spring in Daylesford, Australia. *International Journal of Greenhouse Gas Control*, **84**, 36–46, <https://doi.org/10.1016/j.ijggc.2019.03.003>
- Romeiro-Silva, P.C. and Zalán, P.V. 2005. Contribuição da sísmica de reflexão na determinação do limite oeste do cráton do são francisco. *Simpósio sobre o cráton do são francisco*, 3., 2005, salvador. *Anais. Salvador: sociedade brasileira de geologia*, 44–47.
- Sato, M., Sutton, A.J., McGee, K.A. and Russell-Robinson, S. 1986. Monitoring of hydrogen along the San Andreas and Calaveras faults in central California in 1980–1984. *Journal of Geophysical Research: Solid Earth*, **91**, 12315–12326, <https://doi.org/10.1029/JB091iB12p12315>
- Sherwood Lollar, B., Westgate, T.D., Ward, J.A., Slater, G.F. and Lacrampe-Couloume, G. 2002. Abiogenic formation of alkanes in the Earth's crust as a minor source for global hydrocarbon reservoirs. *Nature*, **416**, 522–524, <https://doi.org/10.1038/416522a>
- Sherwood Lollar, B., Lacrampe-Couloume, G. *et al.* 2006. Unravelling abiogenic and biogenic sources of methane in the Earth's deep subsurface. *Chemical Geology*, **226**, 328–339, <https://doi.org/10.1016/j.chemgeo.2005.09.027>
- Sherwood Lollar, B., Lacrampe-Couloume, G., Voglesonger, K., Onstott, T.C., Pratt, L.M. and Slater, G.F. 2008. Isotopic signatures of CH₄ and higher hydrocarbon gases from Precambrian Shield sites: a model for abiogenic polymerization of hydrocarbons. *Geochimica et Cosmochimica Acta*, **72**, 4778–4795, <https://doi.org/10.1016/j.gca.2008.07.004>
- Sherwood Lollar, B., Onstott, T.C., Lacrampe-Couloume, G. and Ballentine, C.J. 2014. The contribution of the Precambrian continental lithosphere to global H₂ production. *Nature*, **516**, 379–382, <https://doi.org/10.1038/nature14017>
- Stalker, L., Roberts, J., Mabon, L. and Hartley, P.G. 2022. Communicating leakage risk in the hydrogen economy: lessons already learned from geoenery industries. *Frontiers in Energy Research*, <https://doi.org/10.3389/fenrg.2022.869264>
- Sugimoto, A., Inoue, T., Tayasu, I., Miller, L., Takeichi, S. and Abe, T. 1998. Methane and hydrogen production in a termite-symbiotic system. *Ecological Research*, **13**, 241–257, <https://doi.org/10.1046/j.1440-1703.1998.00262.x>
- Sugisaki, R., Ido, M. *et al.* 1983. Origin of hydrogen and carbon dioxide in fault gases and its relation to fault activity. *Geology*, **91**, 239–258, <https://doi.org/10.1086/628769>
- Sukhanova, N.I., Trofimov, S.Y., Polyanskaya, L.M., Larin, N.V. and Larin, V.N. 2013. Changes in the humus status and the structure of the microbial biomass in hydrogen exhalation places. *Eurasian Soil Science*, **46**, 135–144, <https://doi.org/10.1134/S1064229313020142>
- Tarkowski, R. 2019. Underground hydrogen storage: characteristics and prospects. *Renewable and Sustainable Energy Reviews*, **105**, 86–94, <https://doi.org/10.1016/j.rser.2019.01.051>
- Thaysen, E.M., McMahon, S. *et al.* 2021. Estimating microbial growth and hydrogen consumption in hydrogen storage in porous media. *Renewable and Sustainable Energy Reviews*, **151**, 111481, <https://doi.org/10.1016/j.rser.2021.111481>
- Truche, L., Joubert, G., Dargent, M., Martz, P., Cathelineau, M., Rigaudier, T. and Quirt, D. 2018. Clay minerals trap hydrogen in the Earth's crust: evidence from the Cigar Lake uranium deposit, Athabasca. *Earth and Planetary Science Letters*, **493**, 186–197, <https://doi.org/10.1016/j.epsl.2018.04.038>

Natural hydrogen seeps as analogues

- Vacquand, C., Deville, E. *et al.* 2018. Reduced gas seepages in ophiolitic complexes: evidences for multiple origins of the H₂-CH₄-N₂ gas mixtures. *Geochimica et Cosmochimica Acta*, **223**, 437–461, <https://doi.org/10.1016/j.gca.2017.12.018>
- Voitov, G.I., Nikolaev, I.N., Utochkin, Y.A., Rudakov, V.P. and Ishankuliev, D.I. 1995. On the flow of hydrogen into the surface troposphere in geodynamically different geostructural zones of the Earth. *In Dokl RAS*, **344**, 110–114.
- Warr, O., Young, E.D., Giunta, T., Kohl, I.E., Ash, J.L. and Lollar, B.S. 2021. High-resolution, long-term isotopic and isotopologue variation identifies the sources and sinks of methane in a deep subsurface carbon cycle. *Geochimica et Cosmochimica Acta*, **294**, 315–334, <https://doi.org/10.1016/j.gca.2020.12.002>
- Wood, B.L. 1972. Metamorphosed ultramafites and associated formations near Milford Sound, New Zealand. *New Zealand Journal of Geology and Geophysics*, **15**, 88–128, <https://doi.org/10.1080/00288306.1972.10423948>
- Yuce, G., Italiano, F. *et al.* 2014. Origin and interactions of fluids circulating over the Amik Basin (Hatay, Turkey) and relationships with the hydrologic, geologic and tectonic settings. *Chemical Geology*, **388**, 23–39, <https://doi.org/10.1016/j.chemgeo.2014.09.006>
- Zgonnik, V. 2020. The occurrence and geoscience of natural hydrogen: a comprehensive review. *Earth-Science Reviews*, **203**, 103140, <https://doi.org/10.1016/j.earscirev.2020.103140>
- Zgonnik, V., Beaumont, V., Deville, E., Larin, N., Pillot, D. and Farrell, K.M. 2015. Evidence for natural molecular hydrogen seepage associated with Carolina bays (surficial, ovoid depressions on the Atlantic Coastal Plain, province of the USA). *Progress in Earth and Planetary Science*, **2**, 1–31, <https://doi.org/10.1186/s40645-015-0062-5>
- Zgonnik, V., Beaumont, V., Larin, N., Pillot, D. and Deville, E. 2019. Diffused flow of molecular hydrogen through the Western Hajar mountains, Northern Oman. *Arabian Journal of Geosciences*, **12**, 1–10, <https://doi.org/10.1007/s12517-019-4242-2>
- Zimmerman, P.R., Greenberg, J.P., Wandiga, S.O. and Crutzen, P.J. 1982. Termites: a potentially large source of atmospheric methane, carbon dioxide, and molecular hydrogen. *Science (New York, NY)*, **218**, 563–565, <https://doi.org/10.1126/science.218.4572.563>